# University of Alberta

Natural zeolite cracking and light hydrocarbon extraction of bitumen from Athabasca oilsands

by

Haiyan Yin

©

A thesis submitted to the Faculty of Graduate Studies and Research
in partial fulfillment of the requirements for the degree of

Master of Science

in

Chemical Engineering

Department of Chemical and Materials Engineering

Edmonton, Alberta
Fall 2008

Canada

# ABSTRACT

Canada's oilsands is one of the world's largest potential petroleum resources. Different from traditional oil, the bitumen from oilsands has unique problems. The viscosity and concentration of contaminants such as nitrogen, sulfur and heavy metals (especially nickel and vanadium) in the extracted bitumen are much higher than in traditional oil. The industry-dominating water extraction process consumes a huge amount of fresh water for bitumen production. The polluted tailings also create environment issues.

Natural zeolites have been found to have the ability to break down heavy oils into much lighter fractions, and to reduce the viscosity and contaminant levels of the sands. Light hydrocarbon extraction can reduce water consumption and all solvents can be recycled and reused. This study investigated natural zeolite cracking assisted light hydrocarbon extraction of bitumen from Athabasca oilsands. It has been found that natural zeolite cracking significantly improves the bitumen properties. An average of 80% of liquid hydrocarbon samples recovered from natural zeolite cracked products showed a dramatic decrease in the residuum content, indicating the presence of much lighter fractions. About 24% of total nitrogen, 27% of total sulfur and 59% of vanadium content were removed as gas phase products or left in the exhausted sands

# ACKNOWLEDGEMENTS

my dear husband, Yu Feng, for his love, understanding and support, both in the research

and at home, through my two years of M.Sc. life.

## TABLE OF CONTENTS

# LIST OF FIGURES

# CHAPTER 1

# INTRODUCTION

## 1.1 Alberta oilsands mining-extraction industry

Alberta's oilsands are one of the largest potential petroleum resources in the world. The estimated deposit of bitumen is 1.6 trillion barrels.[1] The proven reserve of bitumen is 178 billion barrels, which can be recovered using current technology.[1] Depending on the depth of the proven reserves, about 35 billion barrels can be recovered by the surface mining method and the remaining 143 billion barrels can be recovered by the thermal recovery method.[1]

Alberta's oilsands are located in three major areas: Athabasca, Cold Lake, and Peace River.[2] The Athabasca oilsands deposit is the only one shallow enough to be economical for surface mining. About 10% of the Athabasca oil sands are covered by less than 50 meters of overburden.[3] The Alberta Energy and Utilities Board defined an area of 2,800 square kilometers as the surface mining zone within the Athabasca area.[4]

Initial production began in the 1960s by Great Canadian Oil Sands, (GCOS), now Suncor Energy, Inc. In recent years, higher energy prices, together with significant strides in technology, have made this resource more economical to develop.

A dominant industrial bitumen recovery method for shallow deposits is the Clark Hot Water Extraction (CHWE) process. This was developed in the 1920s by Dr. Karl Clark and is the first commercial extraction process for separating bitumen from the other

constituents of oilsands. This water-based extraction is a process that essentially mixes oilsands with hot water and chemical additives to wash the bitumen out of the sands. The Clark water extraction process recovers bitumen from the sands mainly depending on the hydrophilic properties of oilsands.[5] There is a notion that a thin layer of water surrounds individual sand grains separating them from the bitumen as shown in Figure 1-1.[6-7] Previous research shows that the thickness of the water layer between the sand and bitumen is approximately 10 nm.[8] However, the existence of the water film still needs to be proved by experiments. The hydrophilic property of the Athabasca oilsands makes largely the industrial water-based extraction successful. The water extraction method remains the same after decades as a dominant commercial process, although the hot water temperature has dropped.
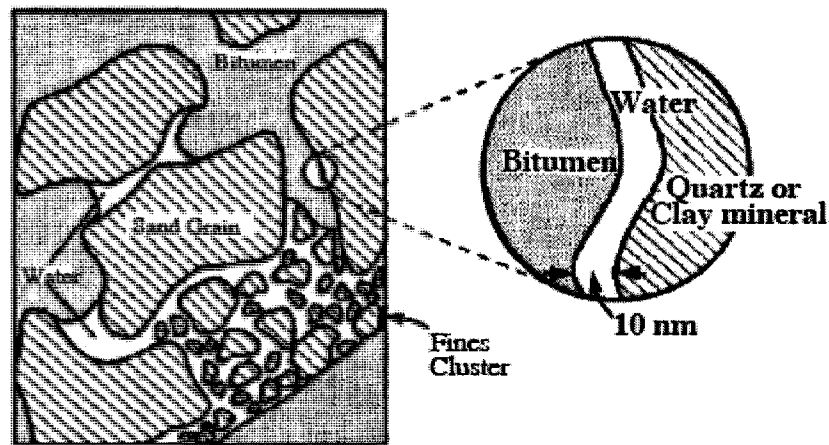


Figure 1-1 The classic model of the structure of Athabasca oilsands[9]

Different companies use different extraction techniques, but the basic steps for water extraction are almost the same, including a mining step, an extraction step and an upgrading step. First, oilsands are mined from the mine ore and crushed. Then, a

mixture of fresh and recycled water mixed with air and chemical additives is added to the oilsands. The slurry is then subjected to mechanical shear to liberate the bitumen. The liberated and aerated bitumen is separated from the sand and water in a primary separation vessel (PSV). The slurry is then separated into three layers in the PSV during the extraction. The top layer is aerated bitumen froth, which contains 60% bitumen, 30% water and 10% solids.[10] The aerated bitumen froth is then de-aerated by steam. Later, naphtha is used to dilute the bitumen froth to reduce its viscosity and centrifuges are used to remove most of the water and solid content from the diluted bitumen. The naphtha is recovered and reused for the next run. The concentrated bitumen is then ready for upgrading. The middle layer is a mixture of bitumen, sands, clay fines and water. The heavy sands drop down to the bottom layer. In the PSV, the bitumen in the middle and bottom layers is recycled again. The exhaust slurries form the tailings, which are transported to the tailing ponds.

## 1.2 Alberta oilsands mining-extraction industry problems

Although Alberta has large oilsands deposits, the bitumen yield of oilsands presents unique problems. Oilsands deposits are composed of sands, clay fines, water and bitumen.[11] Bitumen, the commercially important fraction of the oilsands, has high density and viscosity, which make it unable to flow under gravity at room temperature. Expensive light hydrocarbon solvents must be added to dilute the bitumen before it can be transported through the pipelines to the upgrading facilities. Furthermore, the concentration of contaminants such as sulfur, nitrogen and heavy metals (mainly nickel and vanadium) in bitumen are much higher than in traditional oil.

3

On the other side, compared with oilsands deposits, Alberta's water resource is relatively limited. Alberta has only about 2% of Canada's fresh water.[12] In the oilsands industrial mining extraction process, water is extensively used in hydrotransport, extraction and tailing management. Although mining uses both recycled water and fresh water, multiple cubic meters of fresh water are required to produce a cubic meter of crude oil. With current oilsands industrial development, oilsands mining has already become the largest consumer of water in the Athabasca River basin. In 2005, 76% of the Athabasca River basin's licensed water was consumed by oilsands mining.[13] Long term water usage for oil production raises concerns about both water management and environmental impacts in the Athabasca River basin. With these problems in mind, the mining and water extraction process needs to be improved urgently.

## 1.3 Objectives of the study

Natural zeolites have been known for their ability to break down heavy oil.[14] In this study, economic, single pass natural zeolites were modified and used as catalytic cracking agents to break down the asphaltene molecules in bitumen. The strong adsorption properties of natural zeolites can also potentially help them scavenge a portion of the contaminants such as nitrogen, sulfur and heavy metals.

Organic light hydrocarbon solvents were used instead of water to extract bitumen from raw and cracked oilsands samples. Using light hydrocarbons for extraction reduces water consumption of the process significantly. There are no polluted tailing products in the light hydrocarbon extraction process, so the environmental impact is also reduced. All the light hydrocarbon solvents in the extraction process can be recycled by vacuum

distillation and reused. Considering that catalytic cracking also produces light fractions, the light hydrocarbon solvents can be conceived to be generated in–situ.

The natural zeolite cracking assisted light hydrocarbon extraction of bitumen from Athabsca oilsands is a novel approach to in-field upgrading and bitumen extraction, which can reduce viscosity, contamination and water consumption, and improve the long-term economics of oilsands extraction.

The objectives of this study are:

- To characterize natural zeolites and the different properties that potentially relate to their catalytic cracking ability,

- To investigate the catalytic cracking ability of different types of natural zeolites,

- To investigate the extraction ability of different organic solvents (pentane, hexane and toluene) towards bitumen cracking products.

## 1.4 Background: structure, properties and applications of natural zeolites

### 1.4.1 Natural zeolite framework

The term "zeolite" was derived from two Greek words: zeo ("boils"), and lithos ("stone"). This term initially was used to describe a family of natural minerals that present particular properties: under fast heating conditions, the mineral seemed to boil because of rapid water loss.[15] Natural zeolites have been known for more than two centuries. They are formed in a variety of geological sites and from a variety of precursors, such as volcanic ash, clay, biogenic silica and different forms of quartz.[16]

More than 40 natural zeolites are known; the most common are mordenite, clinoptilolite, chabazite and phillipsite.

Several books give the details of the unique framework of natural zeolites. [17,18,19] For the framework, the primary building units are $TO_4$ tetrahedra (shown in Figure 1-2), where the T-atoms can be Si, Al, P, etc. Adjacent tetrahedra are linked with oxygen atoms. Several $TO_4$ units are connected together to form a chain. Then the chains join together to form rings. The 3-dimensional networks are formed by tetrahedra sharing all four of their corners with other tetrahedra. The natural zeolite framework can be thought to exist as finite or infinite tetrahedral units connecting together. The framework of a natural zeolite contains channels, channel intersections and cages. [20] Inside these voids are water molecules and small cations which compensate for the negative framework charge.



$TO_4$ Tetrahedra     Chain     Ring

Chabazite Framework

Three dimensional

● T atom
◉ O atom
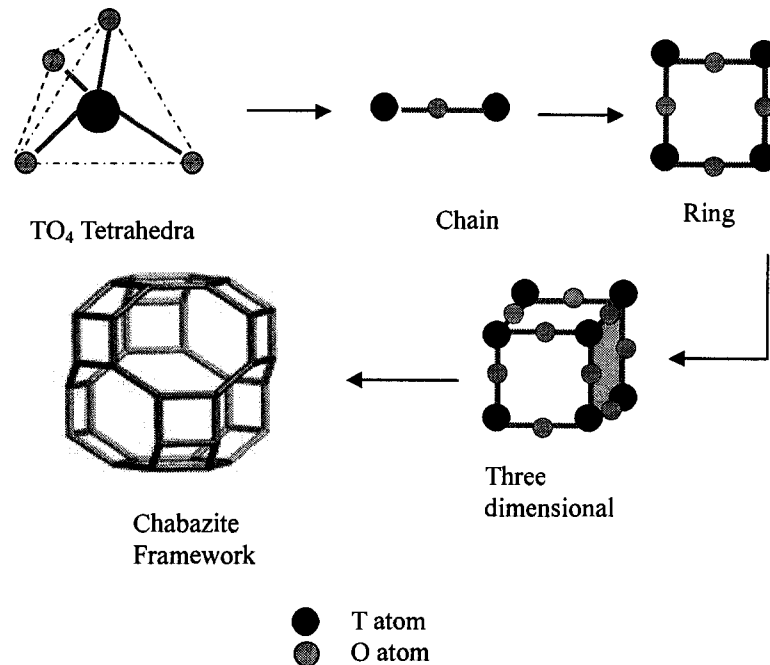
Figure 1-2  Natural zeolite framework[21]

The chemical composition of a natural zeolite can be represented as:

$$A_{y/m}^{m+} [(SiO_2) \, x \, (AlO_2) \, y] \, zH_2O \, [20]$$
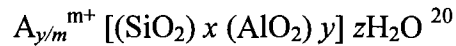
A is a cation with the charge $m^+$. The $y/m$ is the number of cations A per crystallographic unit cell and $z$ is the number of $H_2O$ per crystallographic unit cell. The $x$ is the number of Si tetrahedra per crystallographic unit cell and $y$ is the number of Al tetrahedra per crystallographic unit cell. The $x/y$ is, therefore, the silica to aluminum ratio of the zeolite framework. Lowenstein's rule states that two contiguous aluminum tetrahedra linkages are forbidden, such that $Si/Al \leq 1$. [20]

## 1.4.2 Natural zeolite properties

Natural zeolites have some unique properties that are based on their framework. The framework of natural zeolites contains unique channels and cages; inside these voids are water molecules and small cations. Calcination of natural zeolites dehydrates them and forms channels that can adsorb other molecules. Molecules small enough to enter the natural zeolite cavities will be adsorbed in the channels and larger molecules, which cannot enter the cavities, will be excluded. Adsorption of selected molecules at available sites is affected by the polarity of the adsorbate, electrostatic interaction with the charged zeolite framework, competition with other absorbate molecules, and by both the temperature and pressure of the adsorption process. [22] For all these reasons, natural zeolites have selective adsorption and separation properties.

Natural zeolites have a large internal surface area, which can offer more sites for adsorption. The internal surface area of natural chabazite can reach 450 $m^2/g$. The most important property of natural zeolites is that they have a charged framework. In a natural

zeolite framework, some Si atoms are substituted by Al atoms, resulting in a negatively charged framework. These negative sites are usually balanced by alkaline and alkaline-earth cations, which can be replaced by other cations, thus providing natural zeolites with cation exchange capacity. When alkaline and alkaline-earth cations in natural zeolite structure are substituted for protons, natural zeolites gain acid sites and that can potentially be used as acid cracking catalysts.

### 1.4.3 Applications of natural zeolites

Although there are more than 40 kinds of natural zeolites known, only a few of them such as chabazite, clinoptilolite, erionite, ferrierite, philipsite, mordenite and analcime have sufficient quantity and purity to be considered exploitable resources.[23] In current decades, natural zeolite utilization has been significantly changed because of the growing demand for economical ion-exchange and adsorbent materials in such areas as gas purification and separation, heavy metal recovery and energy application.[24,25,26] Every year, several hundred thousands of tons of zeolitic tuff is mined in the United States, Japan, Italy, Bulgaria, Yugoslavia, Mexico, Korea, and Germany.[27] Natural zeolites have an increasing potential to grow as an important industrial mineral resource.

Adsorption and separation are the dominant applications of natural zeolites. Natural zeolite can be modified to enable separation of heavy metals from waste water by selective adsorption.[28,22] Natural zeolites are also used extensively for commercial gas separation such as air separation, drying of natural gas, hydrocarbon separation, oxygen/argon purification, flue gas/exhaust gas separation and hydrogen/rare gas purification.[24] Ion exchanged natural clinoptilolite was found to be very good for

separation of $N_2$ from $O_2$ and $N_2$ from $CH_4$.[29] The large internal surface area can also potentially make natural zeolite a drug support.[30] In the petrochemical industry, zeolites have the ability to selectively remove hydrocarbons on the basis of molecular size. By using zeolites with channel apertures which accept normal paraffins but not iso-paraffins or aromatics, normal hydrocarbons for detergent manufacture may be separated from hydrocarbons of motor fuel feedstock.[34]

The ability of zeolites to exchange cations is one of the most useful of their characteristics. The low cost of natural zeolites, coupled with exchangeable ions such as innocuous sodium, calcium, and potassium, makes them especially attractive alternatives for removing undesirable heavy metal ions from industrial effluents. The natural zeolites chabazite and clinoptilolite have been investigated for their selectivity and removal performance for the treatment of effluents contaminated with heavy metals such as Pb, Cd, Cu, Zn, Cr, Ni and Co.[31] The removal of ammonia by clinoptilolite from the waste water has also been studied.[32]

The acidic property of natural zeolites plays a major role in zeolitic catalytic materials for acid-catalyzed reactions. The acid catalytic cracking is a very important process in petroleum refining. The main objective of catalytic cracking is to convert high molecular weight hydrocarbon fractions into low molecular weight hydrocarbons. Natural zeolites have been used for catalytic degradation of polymer waste such as polypropylene and polyethylene,[33,34] and are also used for propane dehydrogenation.[35] Modified natural chabazite has been used to crack oilsands bitumen.[14] Several papers have suggested that the catalytic cracking of hydrocarbons over zeolite takes place by bimolecular, monomolecular and oligomeric mechanisms.[36]

[1] National Energy Board, "Canada's Oil Sands: opportunity and challenges to 2015" http://dsp-psd.pwgsc.gc.ca/Collection/NE23-116-2004E.pdf pp 4. (May 2004)

[2] D Woynillowicz, Ch Severson-Baker, M Raynolds, Oil Sands Fever: The Environmental Implications of Canada's Oil Sands Rush, http://pubs.pembina.org/reports/OilSands72.pdf pp 1. (2005)

[3] L. S. Kotlyar, B. D. Sparks, J. R. Woods, Solids Associated with the Asphaltene Fraction of Oil Sands Bitumen, *Energy and Fuels*, Vol.13, pp 346-350. (1999)

[4] D Woynillowicz, C S. Baker, M Raynolds, Oil Sands Fever: The Environmental Implications of Canada's Oil Sands Rush, http://pubs.pembina.org/reports/OilSands72.pdf, pp 2. (2005)

[5] G D. Mossop, Geology of the Athabasca Oil Sands, *Science, New Series*, Vol. 207, No. 4427. pp 145-152. (1980)

[6] K A, Clark, D S. Pastermak, Hot Water Separation of Bitumen from Alberta Bituminous Sand, *Ind. Eng. Chem*, Vol. 24, pp. 1410-1416. (1932)

[7] M W. Ball, Athabasca Oil Sands: Apparent Example of Local Origin of Oil, *Bull. Amer. Assoc. Petroleum. Geol*, Vol. 19, pp.153-171. (1935)

[8] T K. Can, Microscopic Structure of Athbasca Oil Sands, *Chem. Eng. J.*, Vol. 60, pp. 538-545. (1982)

[9] J Czarnecki, B Radoev, L L. Schramm, R Slavchev, On the nature of Athabasca Oil Sands, *Advances in Colloid and Interface Science*, 114–115, pp. 53– 60. (2005)

[10] J Masliyah, Z Zhou, Z Xu, J Czarnecki, and H Hamza, Understanding Water – Based Bitumen Extraction from Athabasca Oil Sand, *The Canadian Journal of Chemical Engineering*, Vol.82, pp. 628-654. (2004)

[11] Q Dai, K H. Chung, Hot water extraction process mechanism using model oil sands, *Fuel*, Vol. 75, No. 2, pp. 220-226. (1996)

[12] http://www3.gov.ab.ca/env/water/gwsw/quantity/waterinalberta/index.html, (Last Review/Updated: September 12, 2005)

[13] "Running out of Steam?", Environmental research and studies center of University of Alberta  http://www.ualberta.ca/~ersc/water.pdf (2007)

[14] S M. Kuznicki, W C. McCaffrey, J Bian, Nature Zeolite bitumen cracking and upgrading, *Microporous and Mesoporous Materials*, Vol.105, pp. 268-272. (2007)

[15] H. Ghobarkar, O. Schäf, U. Guth, Zeolites - from kitchen to space, *Prog. Solid St. Chem.* Vol. 27, pp. 29-73. (1999)

[16] D E.Vaughan, Properties and Applications of Zeolites, Townsend, London, UK. (1980)

[17] J A. Rabo (ed.), Zeolite Chemistry and Catalysis, *American Chemical Society*, Washington, D.C. (1976)

[18] D W. Breck, Zeolite Molecular Sieves, *John Wiley & Sons*, New York. (1974)

[19] A. Dyer, An Introduction to Zeolite Molecular Sieves, *John Wiley and Sons.*, New York. (1988)

[20] J Weitkamp, Zeolites and catalysis, *Solid State Ionics*, Vol. 131, pp. 175–188. (2000)

[21] Ch. Baerlocher, L. B. McCusker, Database of zeolite structure: http://www.iza-structure.org/databases/

[22] E. Alvarez-Ayusoa, A. Garcia-Sanchez, X. Querol, Purification of metal electroplating waste waters using zeolites, *Water Research*, Vol. 37, pp. 4855–4862.( 2003)

[23] S Kesraoui-Ouki, Ch R. Cheeseman, R Perry, Natural Zeolite Utilisation in Pollution Control: A Review of Applications to Metals' Effluents, *J. Chem. Tech. Biortechnol.* Vol. 59, pp. 121-126. (1994)

[24] M W. Ackley, S U. Rege, H Saxena, Application of natural zeolites in the purification and separation of gases, *Microporous and Mesoporous Materials*, Vol.61, pp. 25–42. (2003)

[25] A. A. Zorpas , T. Constantinides, A G. Vlyssides, I. Haralambous, M. Loizidou, Heavy metal uptake by natural zeolite and metals partitioning in sewage sludge compost, *Bioresource Technology*, Vol. 72, pp. 113-119. (2000)

[26] S Ozaydin, G Kocar, A Hepbasli, Natural Zeolites in Energy Applications, *Energy Sources, Part A*, Vol. 28, pp. 1425–1431. (2006)

[27] F. A. Mumpton, Natural zeolites: a new industrial mineral commodity. In Natural Zeolites: Occurrence, Properties, Use,, eds L. B. Sand & F. A. *Mumpton. Pergamon Press*, pp.8-9. (1976)

[28] A. Papadopoulos, D. Fatta, K. Parperis, A. Mentzis, K.-J. Haralambous, M. Loizidou, Nickel uptake from a wastewater stream produced in a metal finishing industry

by combination of ion-exchange and precipitation methods, *Separation and Purification Technology*, Vol. 39, pp. 181–188. (2004)

[29] G Aguilar-Armenta, G Hernandez-Ramirez, E Flores-Loyola, A Ugarte-Castaneda, R Silva-Gonzalez, C Tabares-Munoz, A Jimenez-Lopez, and E Rodriguez-Castellon, Adsorption Kinetics of $CO_2$, $O_2$, $N_2$, and $CH_4$ in Cation-Exchanged Clinoptilolite, *J. Phys. Chem. B* , Vol. 105, pp. 1313-1319. (2001)

[30] A. Rivera , T. Farias, Clinoptilolite–surfactant composites as drug support: A new potential application, *Microporous and Mesoporous Materials*, Vol. 80, pp. 337–346.( 2005)

[31] S K. Ouki, M Kavannagh, Performance of natural zeolites for the treatment of mixed metal-contaminated effluents, *Waste Management & Research*, Vol.15, pp. 383-394. (1997)

[32] E. Cooney, N A. Booker, Ammonia Removal from Wastewaters Using Natural Australian Zeolite. I. Characterization of the Zeolite, *Separation Science and Technology*, Vol. 34(12), pp. 2307–2327. (1999)

[33] E Hwang, J Kim, J Choi, H Woo, D Park, Performance of acid treated natural zeolites in catalytic degradation of polypropylene, *Journal of Analytical and Applied Pyrolysis*, Vol.62, pp.351–364. (2002)

[34] V. Padareva, N. Touleshkov, G. Kirov, Modification of polyethylene with activated natural zeolite, *Journal of Macromolecular Science, Part A Pure and Applied Chemistry*, A35 (7&8), pp. 1079-1091. (1998)


[35] T K. Katranas, A G. Vlessidis, VA. Tsiatouras, KS. Triantafyllidis, N P. Evmiridis, Dehydrogenation of propane over natural clinoptilolite zeolites, *Microporous and Mesoporous Materials*, Vol. 61, pp.189–198. (2003)


[36] Marcelo J. B. Souza, Antonio O. S. Silva, Valter J. Fernandes Jr., Antonio S. Araujo, Catalytic Cracking of $C^{5+}$ Gasoline over HY Zeolite, *React. Kinet. Catal. Lett.*, Vol. 79, No. 2, pp. 257-262. (2003)

# CHAPTER 2

# EXPERIMENTAL SECTION

## 2.1 Oilsands

The oilsands samples employed in this study were obtained from the Syncrude Facility at Mildred Lake near Fort McMurray, Alberta, Canada. The typical asphaltene content of Athabasca bitumen are 17.28-18.8 wt%. [1-2] Carbon, hydrogen, nitrogen and sulfur content are 82.3 wt%, 10.2 wt% 0.47 wt% and 5.05 wt%.[1] The vanadium and nickel concentrations in Athabasca bitumen are approximately 230 ppm and 84 ppm.[1] Oilsands samples were crushed and ground before they were mixed with catalysts.

## 2.2 Catalyst preparation

Commercial zeolite Y, the standard petroleum cracking agent used in this study, was obtained from Engelhard Corporation. As an ammonium-exchanged fluidized catalytic cracking (FCC) microspheres catalyst, pure zeolite Y was ground to a fine powder (<200 mesh) before it was heated to ~450°C under nitrogen flow in a vacuum to convert to the hydrogen form for the acid catalytic cracking reactions.

Raw sedimentary chabazite from the Bowie deposit was acquired from GSA Resources of Tucson, Arizona. The sodium chabazite catalyst used in this study was prepared by the process illustrated in Figure 2-1 and outlined below.

16

```
┌─────────────────┐
│ Raw sedimentary │                              2 times
│ sodium chabazite│      ┌──────────┐      ┌──────────────────┐      ┌──────────────┐
│     (90 g)      │─────┐│ Upgraded │      │    Ammonium      │      │  Calcination │
└─────────────────┘     ││  sodium  │─────▶│    exchange      │─────▶│ (450°C for 1 │
                        ┼│ chabazite│      │ (10 g NH₄NO₃/ 25 g│      │ h, under N₂  │
┌─────────────────┐     ││          │      │ Upgraded chabazite)│      │ and Vacuum)  │
│ Alkaline sodium │─────┘└──────────┘      └──────────────────┘      └──────────────┘
│ silicate solution│
│   (45 g NB+9 g  │
│  NaOH+120 g H₂O)│
└─────────────────┘
```
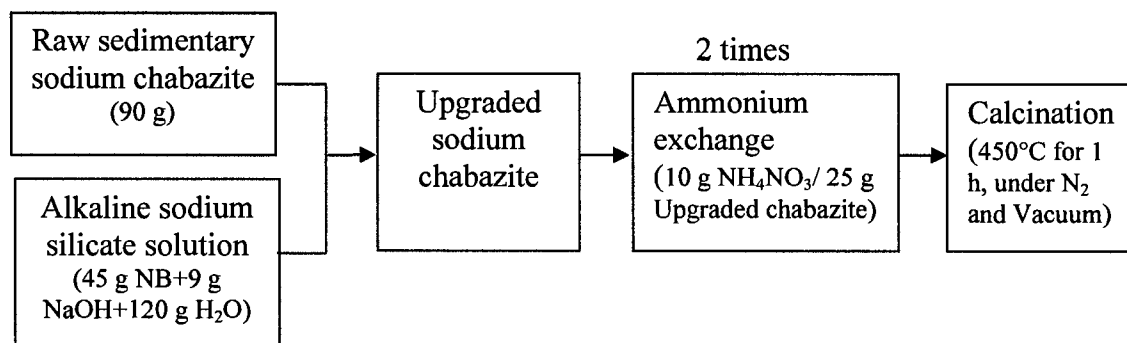
Figure 2-1    Na-Chabazite catalyst preparation process

Natural sedimentary chabazite often contains erionite, epistilbite and clinoptilolite impurity phases. [3] The upgrading process aims to reduce the impure phases and contaminants in the chabazite framework. Upgraded sodium chabazite was prepared by digestion of raw sedimentary chabazite in an alkaline sodium silicate solution. 45 g NB (Sodium silicate solution, obtained from Fisher Scientific) and 9 g NaOH were combined and stirred until the solution became homogenous. 120 g of deionized $H_2O$ was added, and stirring continued until the solution became homogenous again. 90 g of ground (20/50 mesh) raw sedimentary sodium chabazite was added to the alkaline sodium silicate solutions and the mixture was incubated at 60°C for 6-8 h. During the incubation, the mixture was agitated every 30 minutes to keep the chabazite in suspension. After 6-8 h, the mixture was transferred to a 100°C oven and incubated for 16 h without stirring. Next, the chabazite mixture was repeatedly decanted and washed with deionized water until most fines had been removed. Finally, the entire mixture was filtered and dried at 80°C overnight. This product will be referred to as upgraded sodium chabazite.

For many catalytic cracking applications, the Brønsted acid form of a zeolite is required.[4] The Brønsted acid form of zeolite is obtained by introducing ammonium ions, followed by heat treatment, as shown in Equations 2-1and 2-2.[3]

$$\underset{Si}{\overset{\overset{\displaystyle Na^+}{\diagup Al^- \diagdown}}{}} \underset{Si}{\overset{\overset{\displaystyle Na^+}{\diagup Al^- \diagdown}}{}} Si \;+\; 2NH_4NO_3 \rightarrow \underset{Si}{\overset{\overset{\displaystyle NH_4^+}{\diagup Al^- \diagdown}}{}} \underset{Si}{\overset{\overset{\displaystyle NH_4^+}{\diagup Al^- \diagdown}}{}} Si \;+\; 2Na\,NO_3 \qquad\qquad 2\text{-}1$$

$$\underset{Si}{\overset{\overset{\displaystyle NH_4^+}{\diagup Al^- \diagdown}}{}} \underset{Si}{\overset{\overset{\displaystyle NH_4^+}{\diagup Al^- \diagdown}}{}} Si \;\xrightarrow{450^\circ C}\; \underset{Si}{\overset{\overset{\displaystyle H^+}{\diagup Al^- \diagdown}}{}} \underset{Si}{\overset{\overset{\displaystyle H^+}{\diagup Al^- \diagdown}}{}} Si \;+\; 2NH_3\uparrow \qquad\qquad 2\text{-}2$$
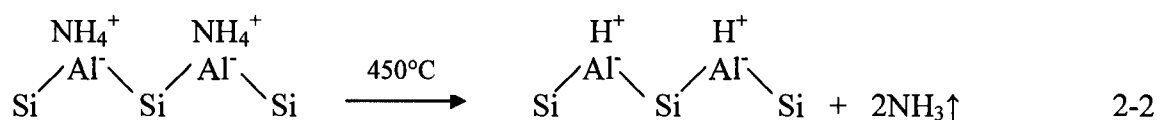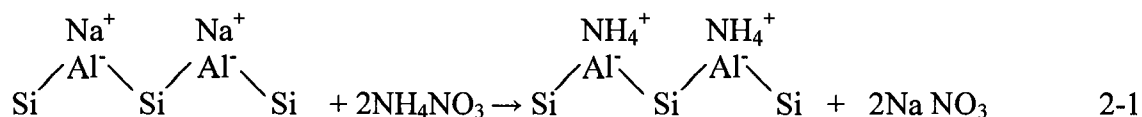
To obtain the Brønsted acid form, upgraded sodium chabazite was subjected to ammonium exchange and calcination. First, upgraded sodium chabazite was ground to a fine powder (<200 mesh). 10 g of ammonium nitrate (Certified ACS, from Fisher Scientific) and 25 g of ground upgraded sodium chabazite were mixed and ~200 mL deionized water was added. The mixture was stirred until the ammonium nitrate dissolved and the solution became homogenous. The pH of the solution was maintained at 3.5-4 by adding a $HNO_3$ solution drop-wise, as required. Ion exchange continued at 80°C for 6-8 h in a water bath with continuous stirring. After 6-8 h, the mixture was decanted, filtered and dried in an oven at 80°C overnight. 25 g of dry ammonium exchanged dried sample was mixed with another 10 g ammonium salts and ~200 mL deionized water and the ammonium exchange process was repeated.

Ammonium exchange was followed by calcination to convert samples to the hydrogen form. Double ammonium-exchanged samples were ground to a fine powder (<200 mesh), loaded into crucibles, and placed in a horizontal isothermal tube furnace.

Samples were heated to 450°C with a 10°C /min heat ramp and held at 450°C for 60 minutes, under a 100 mL/min nitrogen flow in a vacuum. After calcination, the hydrogen form of the sodium chabazite cracking agent was obtained.

Another chabazite cracking agent, calcium chabazite, was prepared by the process illustrated in Figure 2-2.

```
┌─────────────────┐
│ Raw sedimentary │                Ion exchange
│ sodium chabazite│
│     (90 g)      │──┐
└─────────────────┘  │   ┌──────────────┐
                     ├──►│   Upgraded   │          ┌──────────────┐   ┌──────────────┐
┌─────────────────┐  │   │sodium chabazite│────┐   │  Ammonium    │   │ Calcination  │
│ Alkaline sodium │──┘   │    (45 g)    │    │   │  exchange    │   │ (450°C for 1 │
│silicate solution│      └──────────────┘    ├──►│(5 g NH₄NO₃/25 │──►│ h, under     │
│  (45 g NB+9 g   │      ┌──────────────┐    │   │ g Calcium    │   │ N₂ and       │
│ NaOH+120 g H₂O) │      │Calcium chloride│──┘   │ Chabazite)   │   │ Vacuum)      │
└─────────────────┘      │ (45 g + 450 H₂O)│      └──────────────┘   └──────────────┘
                         └──────────────┘
```
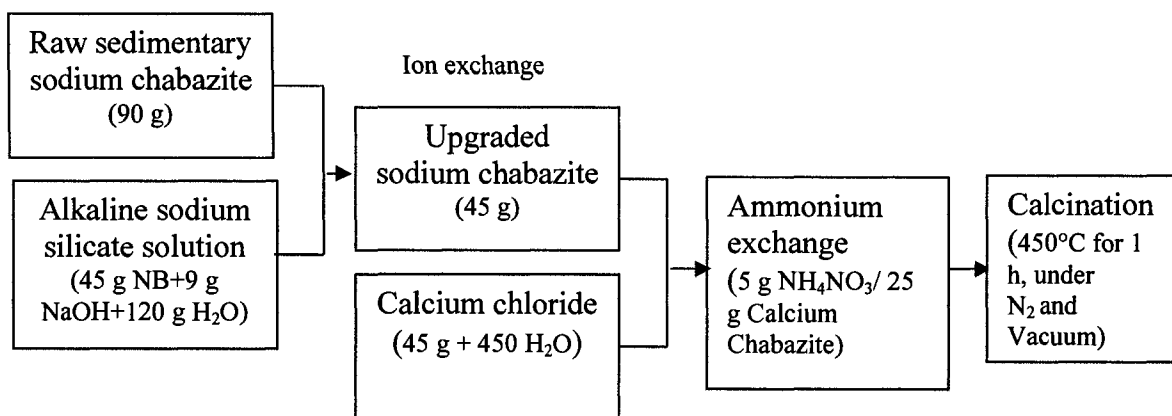
Figure 2-2    Ca-Chabazite catalyst preparation process

The Brønsted acid form of calcium chabazite was made by introducing multivalent metal $Ca^{2+}$ cations (shown in Equations 2-3 and 2-4), followed by the introduction of ammonium ions, followed by heat treatment. [3]

$$\underset{Si}{\overset{Na^+}{\diagup Al^-\diagdown}}\underset{Si}{\overset{Na^+}{\diagup Al^-\diagdown}}Si + [Ca(H_2O)n]^{2+} \rightarrow \underset{Si}{\overset{[Ca(H_2O)n]^{2+}}{\diagup Al^-\diagdown}}\underset{Si}{\overset{}{\diagup Al^-\diagdown}}Si + 2\,Na^+ \qquad 2\text{-}3$$

$$\underset{Si}{\overset{[Ca(H_2O)n]^{2+}}{\diagup Al^-\diagdown}}\underset{Si}{\overset{}{\diagup Al^-\diagdown}}Si \xrightarrow{450°C} \underset{Si}{\overset{[Ca(OH)]^+\quad H^+}{\diagup Al^-\diagdown}}\underset{Si}{\overset{}{\diagup Al^-\diagdown}}Si + (n\text{-}1)\,H_2O \qquad 2\text{-}4$$
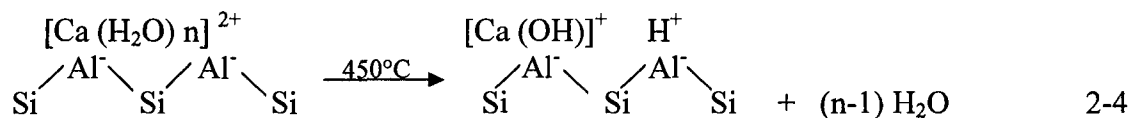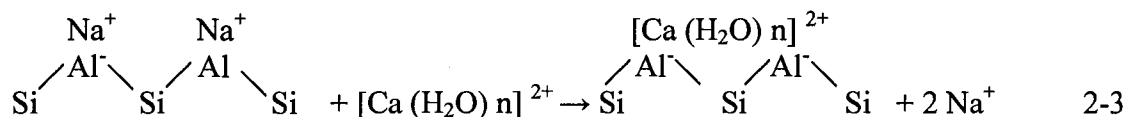
As shown in Figure 2-2, upgraded sodium chabazite was prepared as previously described, followed by ion exchange with calcium chloride. The calcium chloride

solution was prepared by mixing 45 g of calcium chloride and ~450 mL of deionized water and stirring until the calcium chloride was dissolved. 45 g of upgraded sodium chabazite were added and stirring continued until the solution became homogenous. The mixture was incubated at 80°C for 6-8 h and stirred every thirty minutes. After the 6-8 h, the mixture was incubated for another 16 hours without agitation. Next, the mixture was decanted, filtered and dried.

Calcium ion exchange was followed by ammonium ion exchange and calcination to convert the catalyst to the hydrogen form. The ammonium exchange ratio for calcium chabazite was 5 g of ammonium salts to 25 g of ion-exchanged calcium chabazite. The protocol for ammonium exchange and calcination of calcium chabazite was identical to the method used for sodium chabazite.

The natural zeolite cracking agent clinoptilolites were obtained from the Saint Clouds deposit at New Mexico, USA, and from the Werris Creek deposit in New South Wales, Australia. The clinoptilolites were converted to the Brønsted acid form by ammonium exchange followed by heat treatment. Both clinoptilolites were prepared as shown in Figure 2-3. The ammonium exchange ratio is 15 g of ammonium salts to 20 g of clinoptilolites (<200 mesh). The calcination process was identical to that of the protocol used in sodium chabazite.

| Raw Clinoptilolite (New Mexico or Australia) | → | Ammonium exchange (15 g $NH_4NO_3$/ 20 g Clinoptilolite) | → | Calcinations (450°C for 1 h, under $N_2$ and Vacuum) |
| --- | --- | --- | --- | --- |
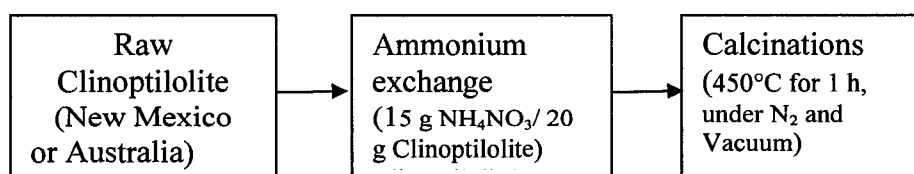
Figure 2-3　Clinoptilolite catalyst prepare process

## 2.3 Catalytic cracking experiments

After the oilsands samples and catalyst samples were prepared, nature zeolite cracking reactions were performed as illustrated in Figure 2-4.

Oilsand (90 wt%)    Catalyst (10 wt%)

Reactor loaded with mixture and sealed

Extraction

Reactor heated in furnace at 350-400°C for 1 h
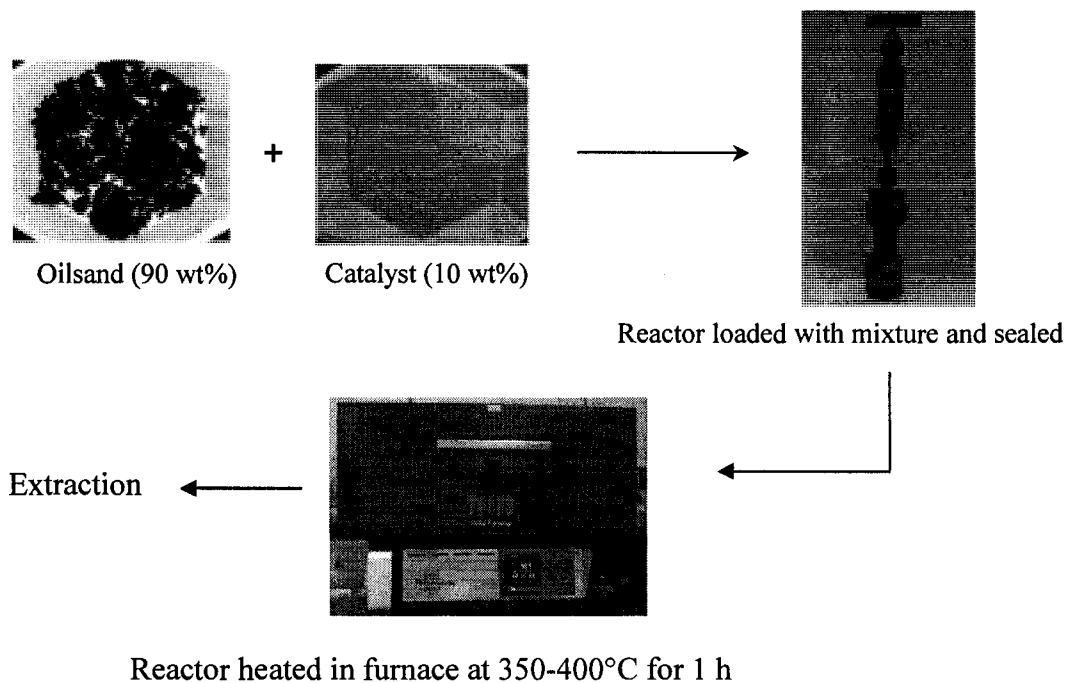
Figure 2-4 Natural zeolite catalyzed cracking reactions

Thermal and catalytic reactions were conducted in micro-batch reactors. Approximately 12 g of raw oilsands (with or without of 1.2 g of 200 mesh catalysts) were ground to form a homogeneous mixture and then loaded into the micro reactor. Leak testing was done under pressure ranging from 200 psi to 270 psi. The nitrogen gas was used to purge the reactor before the reactor was sealed.

The micro reactor then was transferred to a horizontal tube furnace and heated from 25°C to 400°C at a ramp rate of 10 °C/min. The temperature was maintained at 400°C for 1h. After the reaction was complete, the micro reactor was immediately

transferred from the tube furnace to cold water to stop the reaction abruptly. After cooling and drying overnight, the micro reactor was opened in the fume hood. The gas product was measured and released and the solid and liquid products were collected for extraction.

## 2.4 Light hydrocarbon extraction

### 2.4.1 Extraction method

"Once-through" light hydrocarbon extraction was performed in a glass pipette as shown in Figure 2-5. The glass wool in the bottom of the pipette will permit liquid to flow through, while maintaining the solid sands and clay fines.  3 mL of light hydrocarbon solvent (pentane or hexanes) was dripped from the top of the pipette for each extraction and collected for further analysis. After doing the "Once-through" extraction, the exhausted sands were dried and weighted.
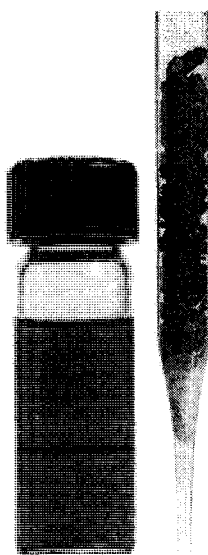


Figure 2-5 "Once-through" extraction

The Reflux extraction equipment is shown in the Figure 2-6. The top of the extraction equipment is a cold water condenser. The middle is a container which can hold the oil sands product thimble. The bottom is a heater and a flask containing the light hydrocarbon solvents. At the beginning of extraction, the heater was adjusted to heat the solvents. When the temperature reached the boiling point of the solvents, the solvents began to evaporate. Then the evaporated solvents condensed in the cold water condenser and dripped into the oil sands thimble to do the extraction. When the extraction solvents in the middle container were full, they fell back to the bottom flasks. This reflux extraction usually lasts 6 hours until all the material can be extracted.
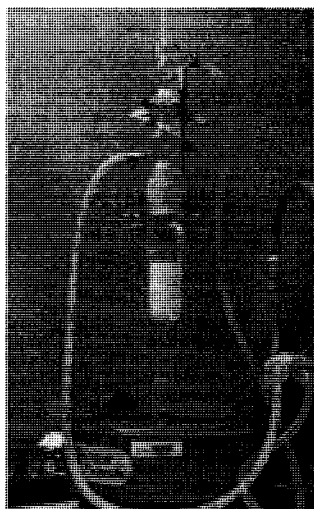


Figure 2-6 Reflux extraction equipment

## 2.4.2 Extraction Experiments

The solid and liquid products obtained from each cracking reaction were transferred to a tray. Approximately 1 g of the solid and liquid products was used for "once-through" extraction. The remaining solid and liquid products were transferred into a porous double thickness extraction thimble. Then the thimble with products was set in

the extraction equipment with 150 mL of the selected light hydrocarbon solvents (pentane or hexanes). After the 6 hour reflux extraction, the solvents were evaporated under a vacuum until the light hydrocarbon solvents were gone. The bitumen was transferred into an aluminum tray, dried for 24 hours, and weighed.

## 2.5 Catalyst characterization

Scanning electron microscopy (SEM) was performed on a JAMP-9500F Auger microprobe (JEOL). An accelerating voltage is 15.0 kV. All samples were coated with carbon prior to SEM analysis.

Phase identification of both raw materials and hydrogen form catalysts was conducted by X-ray powder diffraction (XRD) analysis using a backpack method to ensure random crystal orientation. The samples were analyzed using a Rigaku Geigerflex 2173 with a vertical goniometer equipped with a graphite monochromator for filtration of K-$\beta$ wavelengths

The elemental composition of catalysts was identified using a Hitachi S-2700 scanning electron microscope (SEM) equipped with a PGT (Princeton Gamma-Tech) IMIX digital imaging system and a PG TPRISM IG (Intrinsic Germanium) detector for energy dispersive X-Ray analysis (EDX). All samples were detected under accelerating voltage of 20 kV with a probe current of 2.8 nA.

The Brunauer, Emmett and Teller (BET) method was used to calculate the surface areas of the catalysts. Support surface areas were calculated from nitrogen sorption measurements obtained at 77 K with an Omnisorp 360. Pore size distribution was determined from the desorption branch of nitrogen adsorption isotherms using the

Barrett-Joyner-Halenda formula. Before each adsorption experiment, the sample was out-gassed at 350°C for 4 hours in a vacuum.

The acidity of ammonium bearing catalyst samples was estimated by characterizing thermal decomposition to the hydrogen form. Ammonium TPD (temperature programmed desorption) was carried out using a Netzsch Thermogravimetric Analyzer and Autochem II Micromeritics Chemisorption analyzer for temperature programmed adsorption and desorption (TPA and TPD). Helium was used as the purge and carrier gas.

## 2.6 Product characterization

The recovered liquid hydrocarbon's carbon, hydrogen, nitrogen and sulfur content analysis was conducted on a Carlo Erba EA1108 CHNS-O elemental analyzer.

The recovered liquid hydrocarbon's boiling point was measured by a Netzsch Thermo Gravity Analyzer (TGA). Approximately 10 mg of liquid hydrocarbon sample was loaded into the TGA machine, where the temperature rose from 30°C to 350°C at a ramp of 10 °C/min, then held at 350°C for 20 min. The analysis was done under a vacuum condition.

The concentration of heavy metals (Ni, V) was analyzed by a Perkin Elmer 6000 quadrupole ICP-MS. The liquid samples were prepared by digesting approximately 3 mg of recovered liquid hydrocarbon in a nitric-acid solution for 24 hour at 160°C. Approximately 10 drops of $H_2O_2$ was added to each sample to help the heavy metals in the liquid hydrocarbon dissolve.

[1] T. Gentzis, R.J. Parker, McFarlane R.A, Microscopy of fouling deposits in bitumen furnaces, *Fuel*, Vol. 79, pp. 1173-1184. (2000)

[2] S. Peramanu, B B. Pruden, P. Rahimi, Molecular Weight and Specific Gravity Distributions for Athabasca and Cold Lake Bitumens and Their Saturate, Aromatic, Resin, and Asphaltene Fractions, *Ind. Eng. Chem. Res*. Vol. 38, pp. 3121-3130. (1999)

[3] S M. Kuznicki, C C. H. Lin, J Bian and A Anson, Chemical upgrading of sedimentary Na-chabazite from Bowie, Arizona, *Clay and clay minerals*, Vol. 55, No.3, pp. 235-238. (2007)

[4] J Weitkamp, Zeolite and Catalysis, *Solid State Ionics*, Vol. 131, pp. 175-188. (2000)

# CHAPTER 3

# RESULTS AND DISCUSSION

## Introduction

Economical, single pass natural zeolites, including modified calcium chabazite, have been studied for its ability to catalyze cracking of the bitumen in oilsands.[1] This study investigated different types of natural zeolites as acid catalysts for use in heterogeneous catalytic cracking of bitumen. Several parameters were considered during the selection and preparation of catalysts, including natural morphology, crystal structure and framework Si/ Al ratio. Total surface area and acid strength of the catalysts were also compared. Commercial zeolite Y, raw sedimentary chabazite and natural clinoptilolite were selected for comparison. Zeolite Y, a widely used commercial cracking catalyst, was selected as a reference material. Raw sedimentary chabazite, known to be an effective cracking catalyst in the calcium-exchanged form, was modified in both sodium form and calcium form to investigate the effects of cation selection on cracking capacity. Samples of clinoptilolite, an abundant natural zeolite, were also compared as potential acid catalysts.

## 3.1 Modified natural zeolite characterization

Asphaltenes are large and complex molecules, which constitute a significant portion of bitumen.[1] The molecular weights of Athabasca oilsands asphaltene molecules

often approach 2500 Da.[2] The length and width of typical Athabasca asphaltene molecules are 23-36 Å and 19-23 Å.[2] The surface area of an Athabasca asphaltene molecules is in the range of 2300-2800 Å$^2$ and the volume is approximately 5400 to 6700 Å$^3$.[2] Asphaltenes are such large and complex molecules that they cannot be extracted by light hydrocarbons (pentane or hexanes) unless they are broken down into smaller molecules.

Modified natural zeolite chabazite and clinoptilolite were used as cracking agents to catalyze cracking of the asphaltene molecules and break them down to small molecules that can be extracted by light hydrocarbons (pentane and hexanes). Several properties of natural zeolites, which might be related to catalytic cracking ability, were investigated.

### 3.1.1 Framework and morphology of catalysts

Catalyst morphology was characterized by SEM. Samples were compared to zeolite Y, a common FCC catalyst used to upgrade heavy gas oils to gasoline, diesel fuel, and light gases.[3] The zeolite Y structure consists of truncated octahedral and β cages, tetrahedrally linked through a double six-ring, arranged like the carbon atoms in a diamond (shown in Figure 3-1).[4]
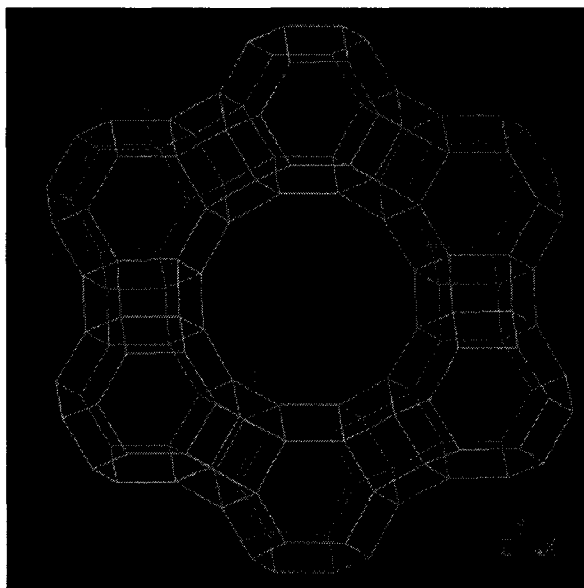
Figure 3-1 Framework of commercial zeolite $Y^5$

In the zeolite Y three-dimensional framework, the free aperture of the twelve-member oxygen rings is 7.4 Å and the free aperture of the super cages is ~13 Å in diameter for each unit cell.[4] The zeolite Y used in this study was obtained from Engelhard Corporation and was already completely ammonium exchanged. It's morphology is shown in Figure 3-2, which might be formed by adding some binders.
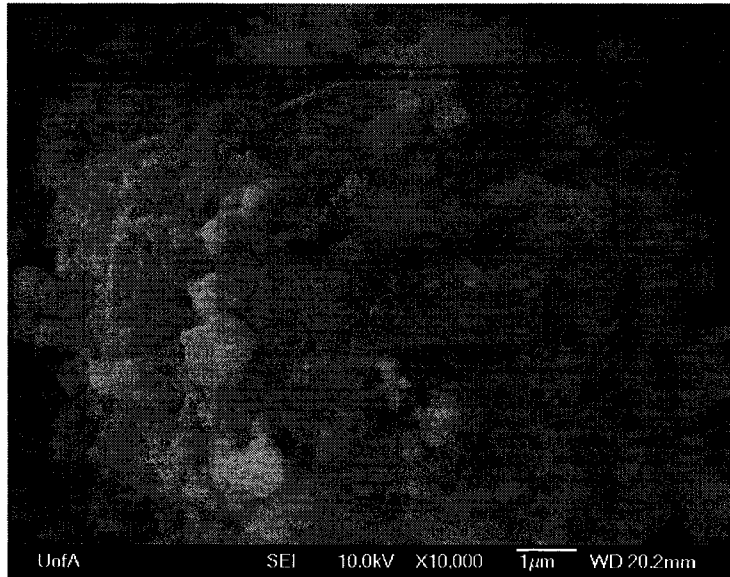
Figure 3-2 SEM image of commercial zeolite Y

Modified mineral chabazite has been demonstrated to catalyze cracking of bitumen in oilsands.[1] The typical framework of chabazite consists of double six-ring (D6R) secondary building units and four-ring enclosed ellipsoidal cages, which combine to generate a three-dimensional channel system.[6] A typical sodium chabazite framework is shown in Figure 3-3.
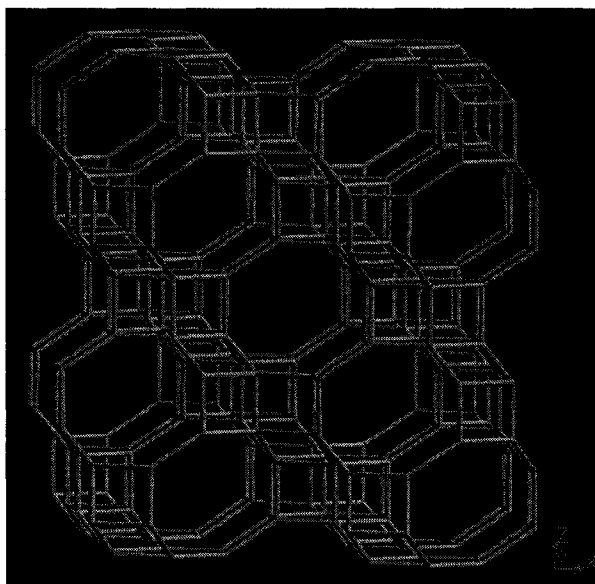
Figure 3-3 Framework of sodium chabazite [5]

The framework Si/Al ratio of natural chabazites ranges from 1.6 to 3.[7] The unit cell constants of chabazite crystal are: a=9.42 Å, β=94°28' and the unit cell volume is 822 Å$^3$.[7] The structure of chabazite has been determined in detail for both dehydrated and hydrated forms.[7] For hydrated chabazite, the free apertures for eight-member rings are 3.7-4.2 Å and for dehydrated chabazite, the free apertures for eight-member rings are 3.1-4.4 Å.[7] Based on the typical structural properties of natural chabazite, large asphaltene molecules will not readily enter the chabazite pores to be cracked within its cages.

The raw sedimentary chabazite used in this study, however, is highly zeolitized Bowie chabazite. Platy morphology is composed of layered crystal in sheets, shown in Figure 3-4. Molecular sieves have catalytic active sites located on both internal pore surfaces and the external surface.[3] Platy morphology, with its increased exterior surface area, permits asphaltene molecules to adsorb on its surface, without entering the chabazite channels.[1] In fact, raw sedimentary chabazite has an exterior surface area slightly in excess of 90 m$^2$/g, a significant part of the total of 500 m$^2$/g.[1]

31
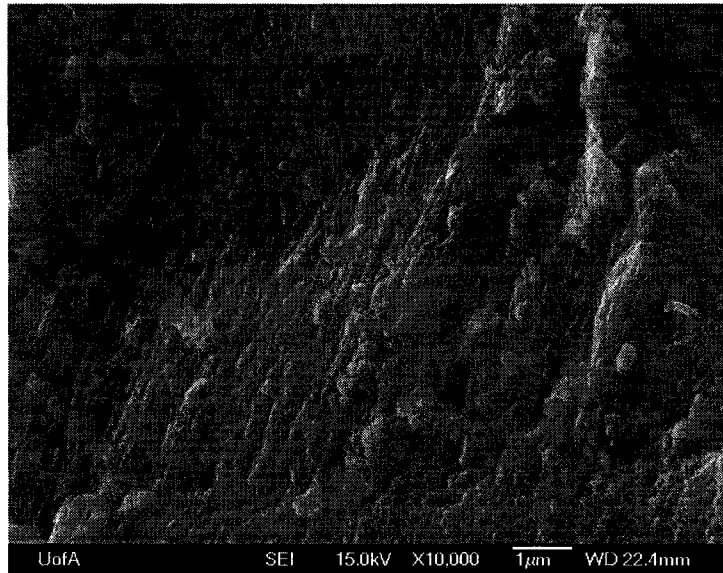
Figure 3-4 SEM image of raw sedimentary chabazite showing platy morphology with high exterior surface area

The Si/Al ratio for the clinoptilolite framework ranges from 4.25 to 5.25.[8] The unit cell constants of clinoptilolite are: a =7.41 Å, b=17.89 Å, c =15.85 Å, $\beta$=91°29' and the unit cell volume is 2100 Å$^3$, larger than the unit cell volume of chabazite. The framework of clinoptilolite is illustrated in Figure 3-5.
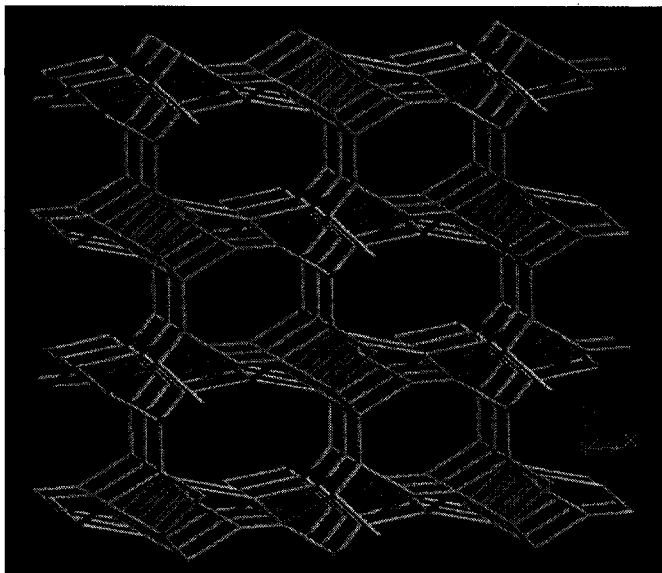
Figure 3-5 Framework of clinoptilolite[5]

The clinoptilolite samples used in this study are highly zeolitized Saint Clouds (New Mexico) and Werris Creek (Australia) samples. Both samples demonstrate platy morphology as shown in Figure 3-6 and 3-7, which, like the morphology of chabazite, results in increased surface areas, permitting large asphaltene molecules to adsorb and be cracked on the clinoptilolite surface.
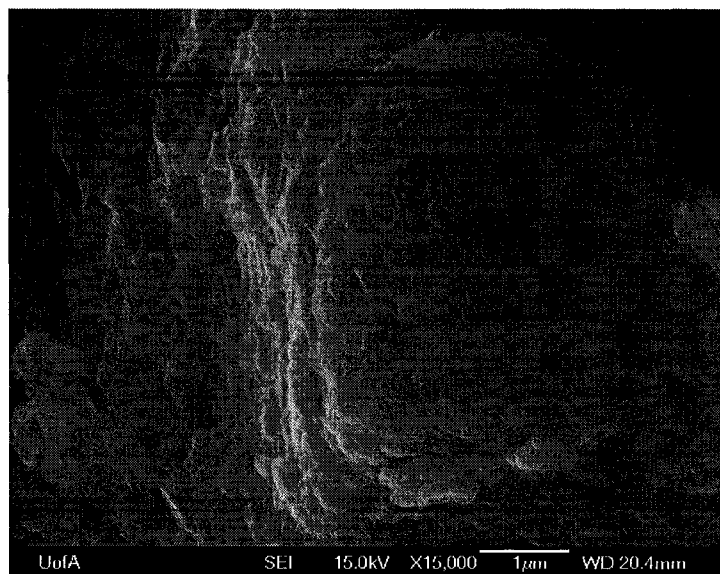
Figure 3-6 SEM image of raw clinoptilolite (New Mexico) showing platy morphology
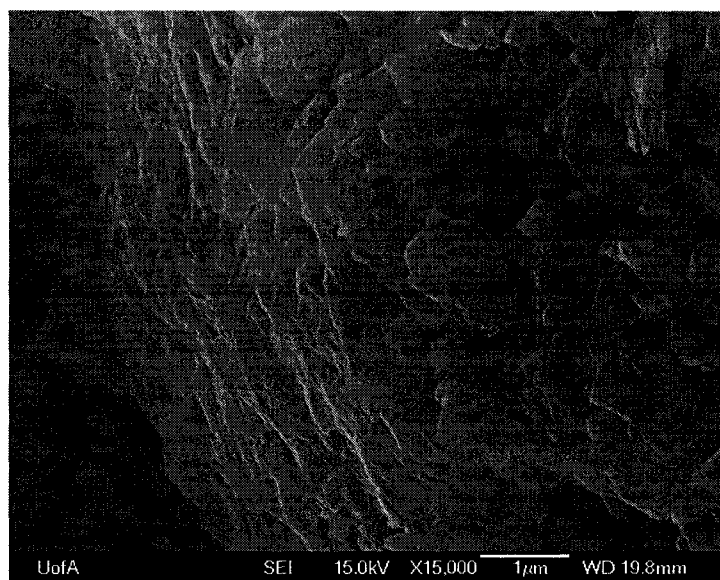


Figure 3-7 SEM image of raw clinoptilolite (Australia) showing platy morphology

## 3.1.2 Crystal structure of catalysts

The crystal structure of the catalysts was characterized by X-ray powder diffraction (XRD). Figure 3-8 shows the XRD patterns for the hydrogen forms of all of

the catalysts used in this work. Commercial zeolite Y is less highly zeolitized than the raw sedimentary chabazite and two clinoptilolite samples used in this study, as is indicated by the less intense reflection peaks.
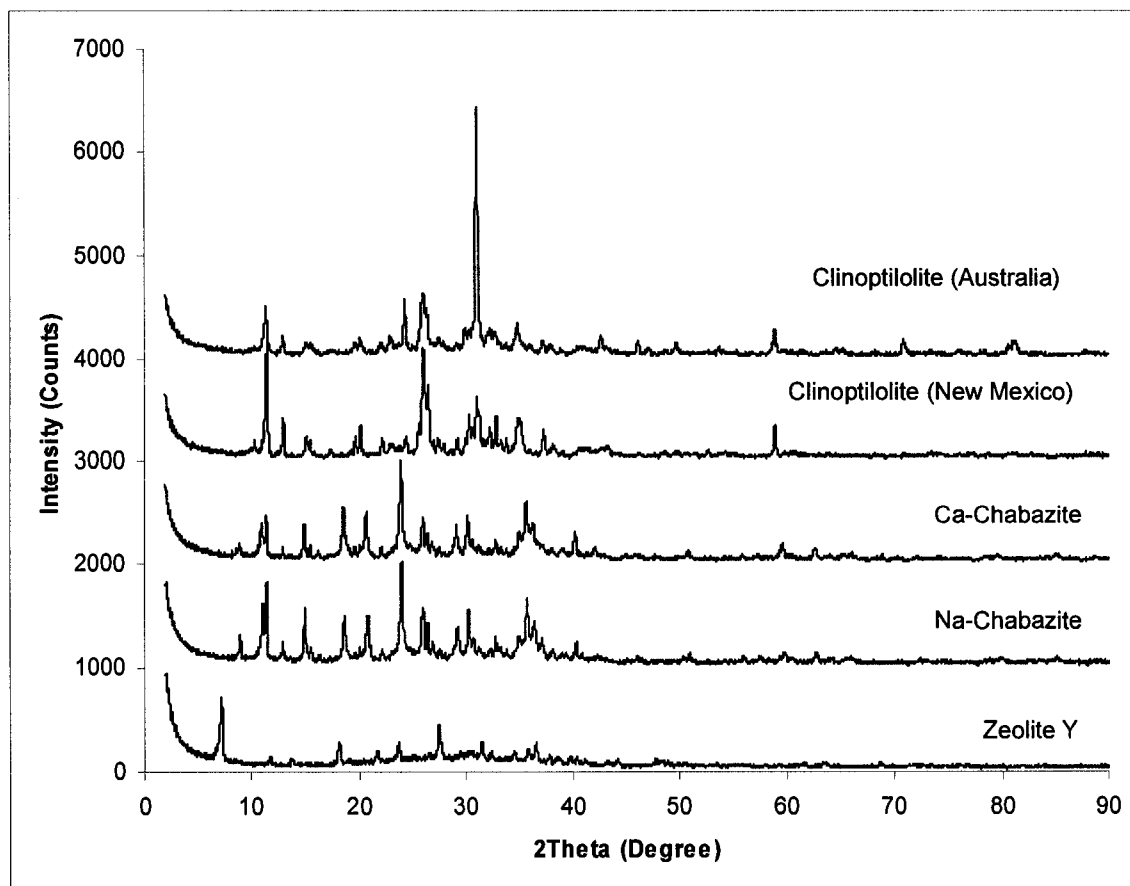


Figure 3-8    XRD patterns for hydrogen forms catalysts

Figure 3-9 shows the XRD patterns of zeolite Y before and after calcination. The results indicate that the zeolite Y framework is unstable. After calcination, the zeolite Y crystal structure is less distinct, indicating distortion of some part of zeolite Y framework following heat treatment.
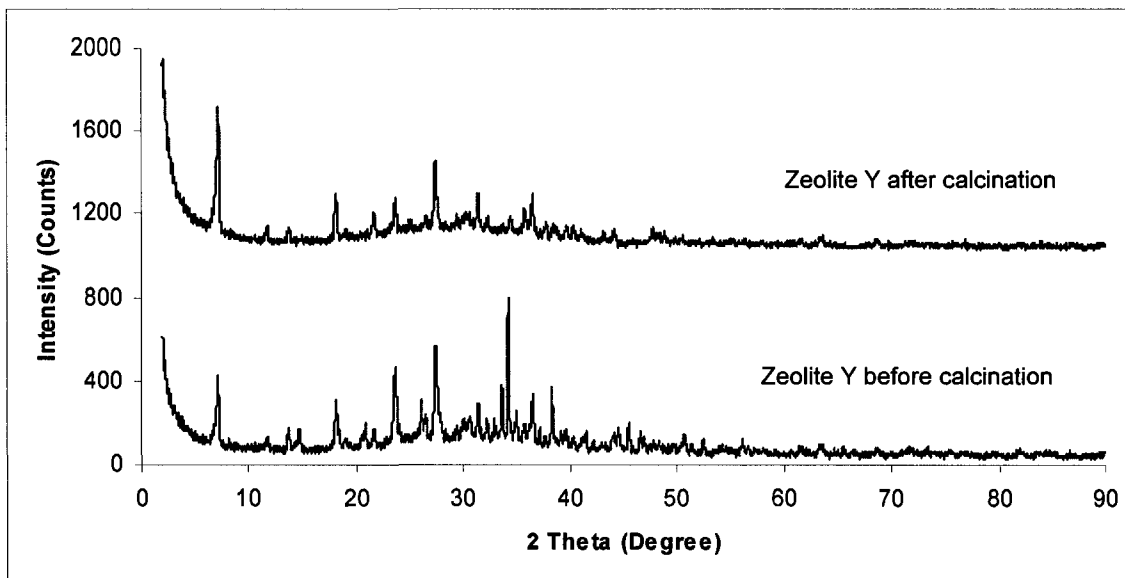
Figure 3-9   XRD patterns for the zeolite Y before and after calcination

Compared with zeolite Y, the XRD patterns indicate that although sodium chabazite and calcium chabazite were prepared by different methods, their crystal structure resembles that of raw sedimentary chabazite after dehydration (Figure 3-10). This indicates that the framework of chabazite is more stable to dehydration than that of zeolite Y.
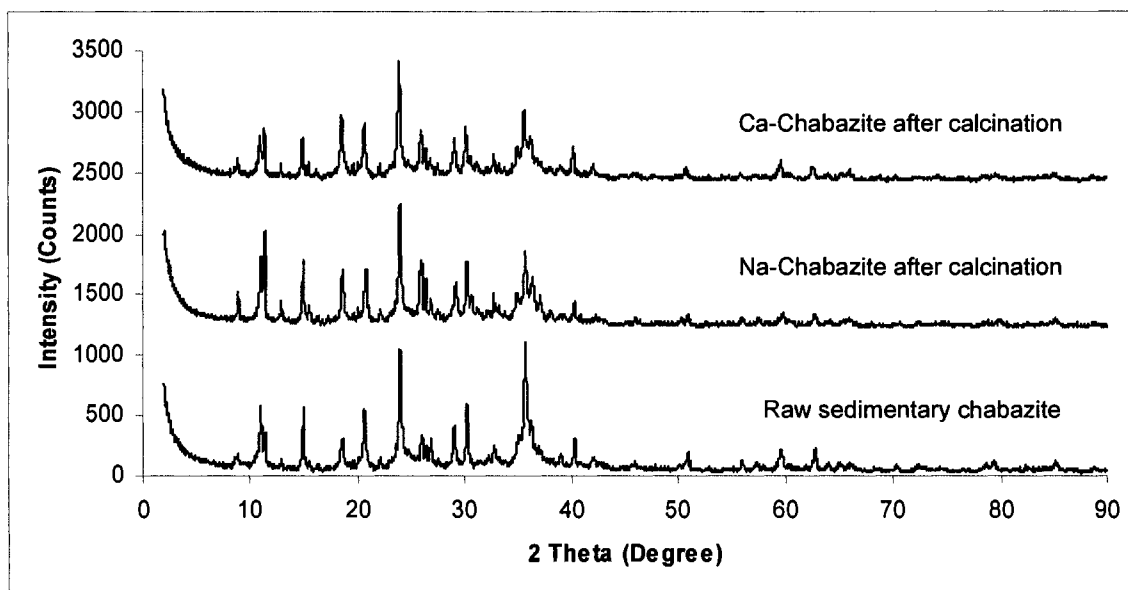
Figure 3-10    XRD patterns for raw and hydrogen forms chabazite catalysts

The clinoptilolite samples from New Mexico and Australia were formed in different environments and the XRD patterns indicate that the two clinoptilolite samples contain different impure phases (shown in Figure 3-11). The XRD patterns also indicate that the clinoptilolite from New Mexico contains more impurities than the Australian one. The XRD patterns illustrate there is no discernable difference between raw clinoptilolite samples and their calcined forms, indicating that the clinoptilolite framework is more stable during calcination than either chabazite or zeolite Y.

7000

6000

5000

4000

3000

2000

1000

0

Intensity (Counts)

Modified   clinoptilolite (Australia)

Raw clinoptilolite (Australia)

Modified clinoptilolite (New Mexico)

Raw clinoptilolite (New Mexico)

0    10    20    30    40    50    60    70    80    90

2 Theta (Degree)
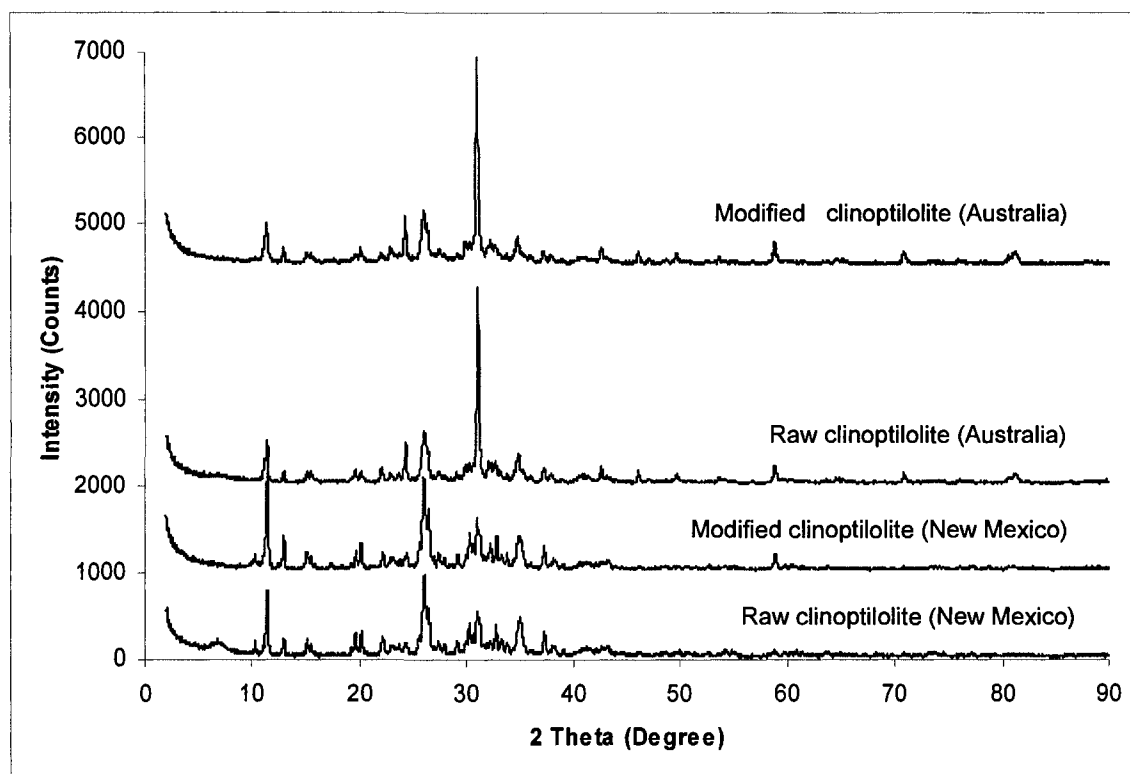
0

Figure 3-11    XRD patterns for raw and hydrogen form clinoptilolite catalysts

### 3.1.3 Total surface area and pore size distribution of catalysts

The surface area of the catalyst was measured by the Brunauer, Emmett and Teller (BET) method (Table 3-1). The total surface area of commercial zeolite Y is 267 $m^2/g$. The meso and macropore surface area is 77 $m^2/g$. The calcium chabazite total surface area is 419 $m^2/g$. Although calcium chabazite has a higher total surface area, its meso and macroporous area is lower (59 $m^2/g$). The sodium chabazite total surface area is 417 $m^2/g$, while the meso and macroporous area is 48 $m^2/g$. For clinoptilolites from New Mexico and Australia, the total surface area is about 100 $m^2/g$ and the meso and macropore area is about 40 $m^2/g$.

Table 3-1 BET surface area of hydrogen form zeolite Y, Ca-chabazite, clinoptilolite
(New Mexico) and clinoptilolite (Australia)

| Catalyst Samples | Total surface area (m$^2$/g) | Meso and macropore (m$^2$/g) |
|---|---|---|
| Zeolite Y | 267 | 77 |
| Na-chabazite | 417 | 48 |
| Ca-Chabazite | 419 | 59 |
| Clinoptilolite (New Mexico) | 101 | 40 |
| Clinoptilolite (Australia) | 99 | 44 |

From the BET pore size distribution (Figure 3-12), the two clinoptilolites have quite uniform mesopores, with pore radii varying from 15 Å to 20 Å. Sodium, calcium chabazite and zeolite Y have more meso and macropores, but they are distributed over the whole size range (15 Å ~200 Å).
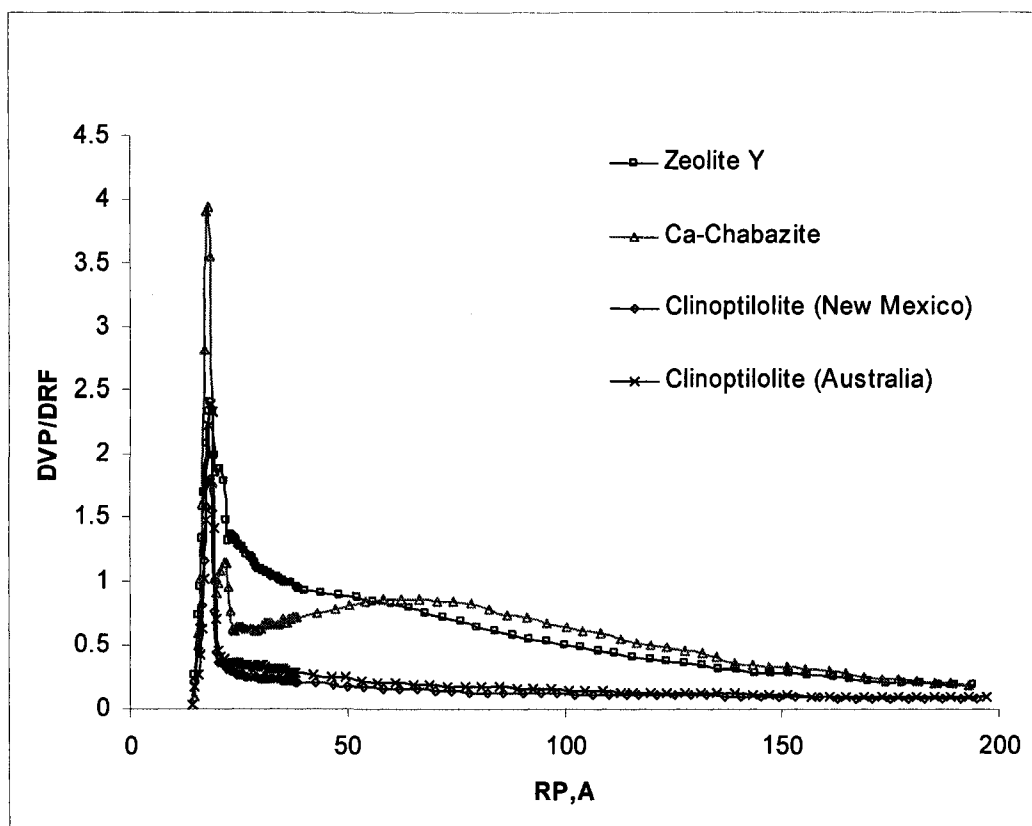
Figure 3-12 Pore size distribution

### 3.1.4 Chemical composition of catalysts

The chemical composition of the catalysts was investigated by energy dispersive X-ray (EDX) analysis (Table 3-2). Commercial zeolite Y has the lowest observed Si/Al ratio (2.4), while chabazite has a higher Si/Al ratio, that is, between 3.5 and 3.7. Clinoptilolite has the highest Si/Al ratio, ranging from 5.0 to 5.1. Aluminum ions in the zeolite framework are not as stable as silica ions at high temperature. The aluminum ions become unstable and migrate out of the framework, which may induce zeolite framework distortion. For natural chabazite, dehydration results in some framework distortion.[8] Clinotilolite, with its higher Si/Al ratio, is more stable (the framework can withstand

40

calcination at 700°C in air). The stable structure and abundant acid sites in clinoptilolite may make the catalysts more stable during high temperature catalytic cracking reactions.[8]

Table 3-2 Si/Al ratio of catalysts measured by EDX

| Catalyst | Si/Al ratio |
| --- | --- |
| Zeolite Y | 2.4 |
| Na-chabazite | 3.7 |
| Ca-chabazite | 3.5 |
| Clinoptilolite (New Mexico) | 5.0 |
| Clinoptilolite (Australia) | 5.1 |

For chabazite catalysts, EDX analysis indicates that alkaline sodium silicate upgrading process removes contaminants from raw sedimentary chabazite. The upgrading process reforms the impurities found in the raw sedimentary chabazite framework (Mg, S and Cl; Table 3-3). The results of elemental analysis indicate that the formation of Brønsted acid sites in sodium chabazite is largely ammonium induced, while the formation of Brønsted acid site in calcium chabazite is largely calcium ion induced.

Table 3-3 EDX elemental analysis of raw sedimentary chabazite, Na-chabazite and Ca-chabazite

| Sample name<br><br>Elements | Raw sedimentary<br>chabazite<br>(wt%) | Na chabazite<br>Upgraded<br>(wt%) | Ca chabazite<br>Upgraded<br>(wt%) |
|:---:|:---:|:---:|:---:|
| Na | 7.15 | 0 | 0 |
| Ca | 0 | 0 | 3.38 |
| Mg | 0.75 | 0 | 0 |
| S | 0.39 | 0 | 0 |
| Cl | 0.28 | 0 | 0 |

All of the sodium in sodium chabazite was replaced by ammonium after ammonium exchange (two times). During calcination, most of the ammonium was thermally decomposed to ammonia to form Brønsted acid sites, while ammonia gas was carried out by nitrogen flow in the vacuum. For calcium chabazite, calcium chloride ion exchange converts more than 90% of the sodium sites to calcium cation sites. After partial ammonium exchange and calcination, Brønsted acid sites were formed in calcium chabazite, mainly as a result of cation exchange.

EDX elemental analysis shows that after full ammonium exchange and calcination, the concentration of some cations in clinoptilolite (New Mexico), such as $Mg^{2+}$ and $Ca^{2+}$, decreased (Table 3-4). The $Mg^{2+}$ concentration was reduced by 0.32% and $Ca^{2+}$ concentration was reduced by 2.30%. For the Australian clinoptilolite sample, the $Mg^{2+}$ concentration was reduced by 0.77%, $Ca^{2+}$ concentration was reduced by 2.31% and $K^{+}$ concentration was reduced by 0.52%. The EDX results illustrate that ammonium exchange replaced both monovalent and divalent cations.

Table 3-4 EDX elemental analysis of raw clinoptilolite (New Mexico and Australia), and modified clinoptilolite (New Mexico and Australia).

| Sample name Elements | Raw Clino (New Mexico) (wt%) | Modified Clinoptilolite (New Mexico) (wt%) | Raw Clino (Australian) (wt%) | Modified Clinoptilolite (Australian) (wt%) |
|---|---|---|---|---|
| Mg | 1.43 | 1.01 | 1.26 | 0.49 |
| K | 2.44 | 2.25 | 2.36 | 1.84 |
| Ca | 2.94 | 0.64 | 2.88 | 0.57 |

### 3.1.5 Catalyst acid site density

The density of acid sites in zeolites is related to framework aluminum content. By comparing EDX results for aluminum concentration, we can estimate the concentration of acid sites by assuming that each $H^+$ site corresponds to one Al atom.[9] An estimate of total acid sites and their distribution is shown in Table 3-5.

Table 3-5 Total number of acid site density for the catalysts in their hydrogen form

| Sample Name (Hydrogen form) | Si/Al ratio | Calculated [Al⁻] concentration mmol/g | Total cations mmol/g | Potential maximal [H⁺] mmol/g | Total surface area $m^2/g$ | Average acid site density mmol/$m^2$ |
|---|---|---|---|---|---|---|
| Zeolite Y | 2.4 | 6.0 | 3.4 | 2.6 | 267 | 0.0098 |
| Na-chabazite | 3.7 | 5.1 | 1.3 | 3.8 | 417 | 0.0091 |
| Ca chabazite | 3.5 | 4.7 | 2.6 | 2.1 | 419 | 0.0050 |
| Clinoptilolite (New Mexico) | 5.0 | 3.8 | 2.4 | 1.4 | 101 | 0.014 |
| Clinoptilolite (Australia) | 5.1 | 3.7 | 1.9 | 1.8 | 99 | 0.018 |

As the Si/Al ratio increases, the aluminum concentration in the catalyst framework decreases (Table 3-5). The framework aluminum concentration in commercial zeolite Y is about 6.0 mmol/g, indicating that after ammonium exchange and calcination, there are 6.0 mmol/g of potential aluminum sites on the zeolite Y framework. Of the aluminum sites, approximately 3.4 mmol/g are associated with cations and 2.6 mmol/g may be associated with $H^+$. Based on a total measured surface area of zeolite Y of 267 $m^2$/g, the average acid site density of zeolite Y was calculated to be 0.0098 mmol/$m^2$. For sodium chabazite, the total potential aluminum sites in the framework after calcium exchange were 5.1 mmol/g; approximately 1.3 mmol/g were associated with cations and 3.8 mmol/g may be related with $H^+$. Based on the total surface area (417 $m^2$/g) of sodium chabazite, the average acid site density of sodium chabazite was calculated to be 0.0091 mmol/$m^2$. For calcium chabazite, the total potential aluminum sites in the framework after calcium exchange were 4.7 mmol/g; approximately 2.6 mmol/g were associated with cations and 2.1 mmol/g may be related with $H^+$. Based on the total surface area (419 $m^2$/g) of calcium chabazite, the average acid site density of calcium chabazite was calculated to be 0.005 mmol/$m^2$. For clinoptilolite (New Mexico), the catalyst has approximately about 3.8 mmol/g of potential aluminum sites; 2.4 mmol/g sites associated with cations and 1.4 mmol/g potentially related with $H^+$. Combined with its total surface area (101 $m^2$/g), the calculated average acid site density of clinoptilolite (New Mexico) was 0.014 mmol/$m^2$. For clinoptilolite (Australia), there were approximately 3.7 mmol/g of potential aluminum sites on the catalyst framework; 1.9 mmol/g associated with cations and 1.8 mmol/g potentially related with $H^+$. Combined with its total surface area

(99 $m^2/g$), the calculated average acid site density of clinoptilolite (Australia) was 0.018 $mmol/m^2$.

From calculated average framework acid site density, the clinoptilolite samples have higher densities of acid sites than zeolite Y and chabazite. Clinoptilolite (Australia) has the highest acid site density among all of the catalysts tested.

### 3.1.6 Catalyst acid strength

Catalyst acid strength was characterized by ammonia TPD. Figure 3-13 shows the TPD profile of reversibly adsorbed ammonia on different natural zeolites. Table 3-6 summarizes the temperature for ammonia desorption peaks. Table 3-7 outlines the distribution of acid sites on the catalyst surface as determined by peak fit simulation.
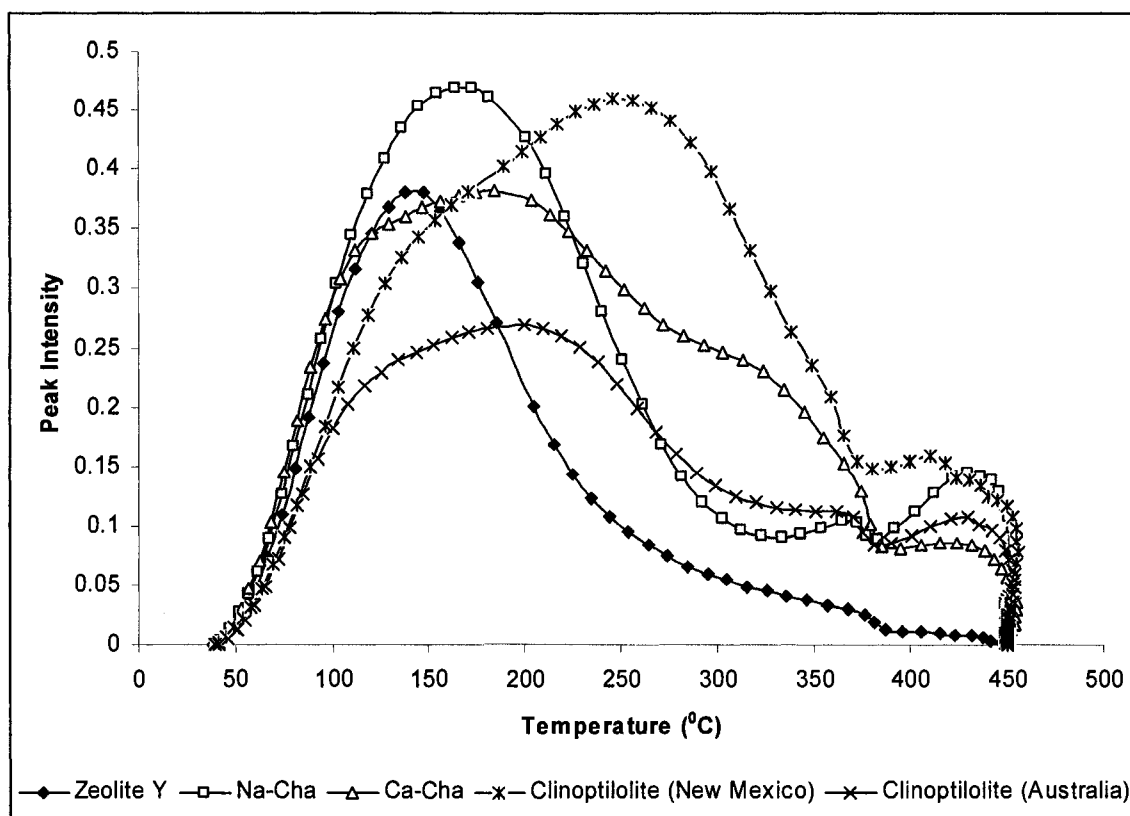
Figure 3-13 Ammonia TPD spectra of zeolite Y, Na-chabazite, Ca-chabazite, clinoptilolite (New Mexico) and clinoptilolite (Australia):

Temperature ramp rate, 30 °C/min; Helium flow: 30 cm$^3$/min.

Table 3-6 Ammonia TPD spectra for zeolite Y, Na-chabazite, Ca-chabazite, clinoptilolite (New Mexico) and clinoptilolite (Australia)

| Catalyst Sample | Temperature of weak adsorption (°C) | Temperature of medium adsorption (°C) | Temperature of strong adsorption (°C) |
|---|---|---|---|
| Zeolite Y | 142 | 373 | - |
| Na Chabazite | 162 | 367 | 428 |
| Ca Chabazite | 110, 192 | 312 | 432 |
| Clinoptilolite (New Mexico) | 128 | 249 | 414, 434 |
| Clinoptilolite (Australia) | 191 | 369 | 427 |

Table 3-7 Acid site distribution form ammonia TPD desorption

| Catalyst Sample | Area of weak adsorption (%) | Area of medium adsorption (%) | Area of strong adsorption (%) |
|---|---|---|---|
| Zeolite Y | 93 | 7 | 0 |
| Na Chabazite | 90 | 6 | 4 |
| Ca Chabazite | 71 | 27 | 2 |
| Clinoptilolite (New Mexico) | 28 | 69 | 3 |
| Clinoptilolite (Australia) | 91 | 4 | 5 |

From the ammonia TPD profile, zeolite Y has two desorption peaks centered at 142°C and 373°C. The 142°C peak is related to the weak adsorption of ammonia and the 373°C peak is related to the medium adsorption. About 93% of the total acid sites were located in the weak adsorption area and only 7% of the total acid sites were associated with the medium adsorption sites. This result indicates that zeolite Y has a weak acid strength.

Sodium chabazite has three desorption peaks centered at 162°C, 367°C and 428°C. The 162°C peak is related to the weak adsorption and the 367°C peak is related to the medium adsorption and the 428°C peak is related to the strong adsorption. About 90% of the total acid sites were located in the weak adsorption area and 6% of the total acid sites were associated with the medium adsorption area. The strong adsorption area was estimated to be 4%. From this result, sodium chabazite has stronger adsorption sites than zeolite Y.

Calcium chabazite has four desorption peaks centered at 110°C, 192°C and 312°C, 492°C. Both the 110°C and 192°C peaks are related to the weak adsorption area and the 312°C peak is related to the medium adsorption area, while the 432°C peak is related to the strong adsorption area. About 71% of the total acid sites were located in the weak adsorption area and 27% of the total acid sites were located in the medium adsorption area. The strong adsorption area is 2%. Calcium chabazite has more medium adsorption area than sodium chabazite. The total adsorption area of calcium chabazite is also larger than that of sodium chabazite, which indicates that multiple cation induced Brønsted acid sites have a higher acid strength than ammonium induced Brønsted acid sites.

Clinoptilolite (Australia) has three desorption peaks centered at 191°C, 369°C and 427°C. The 191°C peak is related to the weak adsorption area and the 369°C peak is related to the medium adsorption area. The 427°C peak is related to a strong adsorption area. The weak adsorption area (91%) in clinoptilolite (Australia) is slightly smaller than the weak adsorption area of zeolite Y, medium (4%) and strong adsorption areas (5%) are large than those of zeolite Y, based on these results; clinoptilolite (Australia) has stronger acid strength than zeolite Y.

Clinoptilolite (New Mexico) also has four desorption peaks centered at 128°C, 249°C and 414°C, 434°C. The 128°C peak is related to the weak adsorption area and the 249°C peak is related to the medium adsorption area. Both the 414°C and 432°C peaks are related to a strong adsorption area. The clinoptilolite (New Mexico) has the largest total adsorption area. The weak adsorption area in clinoptilolite (New Mexico) is 28% of the total adsorption area, which is dramatically lower than the fraction of weak adsorption in zeolite Y and chabazite.   Clinoptilolite (New Mexico) also has the largest medium

48

adsorption area, which occupies 69% of the total area. In addition, clinoptilolite (New Mexico) has 3% of strong adsorption area. From the results, clinoptilolite (New Mexico) has the sites of greatest acid strength for all the examined catalysts.

## 3.2 Characterization of recovered liquid hydrocarbon samples

### 3.2.1 Cracking and liquid hydrocarbon recovery

The results of once-through pentane extraction from raw oilsands, thermally cracked and clinoptilolite-cracked oilsands samples are shown in Figure 3-14. Visual comparison of the exhausted sands and recovered liquid indicates that the natural clinoptilolite is an effective cracking catalyst. The sand from the pentane-extracted raw oilsands sample maintains most of its initial structure and color. In sharp contrast, the extraction of the clinoptilolite-cracked sample leaves the sands exhausted and collapsed. The sand from the thermally cracked sample displays an intermediate structure and color. The liquid from the thermally cracked sample has the lightest color; in contrast, the liquid collected from the natural clinoptilolite-cracked sample shows a deep brown color, indicating that the cracking has resulted in a readily extractable product. The bitumen liquid collected from the raw oilsands shows an intermediate color between thermal cracking and clinoptilolite cracking.
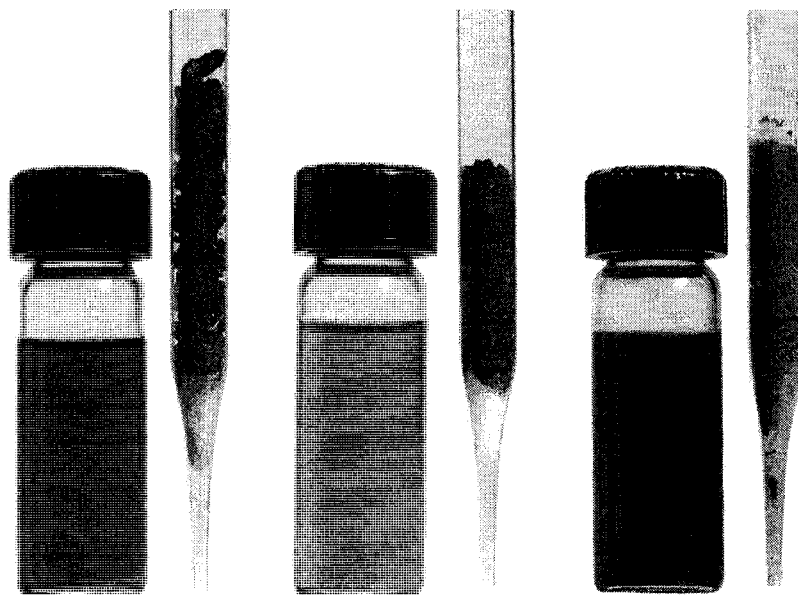
Figure 3-14 Oilsand samples extracted using pentane: raw (left); thermally cracked (middle) and nature clinoptilolite cracked (right).

Table 3-8 shows the weight percentage of liquid hydrocarbon recovered from pentane-, hexane- and toluene-extracted raw and cracked oilsands samples. The result shows natural zeolite clinoptilolite-cracked oilsands samples have a high liquid hydrocarbon recovery rate by pentane extraction. In pentane extracted raw and cracked oilsands samples, the highest weight percentage of liquid hydrocarbon is recovered from the clinoptilolite (New Mexico)-cracked oilsands sample, which is 85 wt%. In comparison, the raw, thermally-cracked and zeolite Y-cracked samples have recoveries of 72, 77 and 77 wt% of liquid hydrocarbon respectively. However, despite room temperature leak-testing of micro reactors at 270 psi, one cannot exclude the possibility that some light liquid hydrocarbon products were still lost due to very high pressure build-up during the clinoptilolites catalytic cracking reactions. When hexane is used as the extraction solvent, thermally cracked and raw oilsands yield higher bitumen

recoveries (86 and 79 wt%, respectively) than the clinoptilolite cracked samples (69 and 76 wt%).

Toluene extraction had a higher liquid hydrocarbon recovery than pentane or hexane extraction; however, toluene is known to co-extract the asphaltenes remaining within the bitumen, which is undesirable for upgrading.

Table 3-8 The effect of catalysts and extraction solvents on liquid hydrocarbon recovery from oilsands samples

| Cracked oilsands sample | Liquid hydrocarbon recovery (wt %) | | |
| --- | --- | --- | --- |
| | Pentane extracted | Hexane extracted | Toluene extracted |
| Raw oilsands | 72 | 86 | 100 |
| Thermal cracking | 77 | 79 | 85 |
| Zeolite Y | 77 | 79 | 89 |
| Na-chabazite | 83 | 79 | 88 |
| Ca-chabazite | 73 | 65 | 97 |
| Clinoptilolite (New Mexico) | 85 | 69 | 78 |
| Clinoptilolite (Australia) | 74 | 76 | 79 |

### 3.2.2 Thermal gravimetric analysis of recovered liquid hydrocarbon samples

Vacuum-distillation curves of the recovered liquid hydrocarbon samples were recorded using a Netzsch Thermogravimetric Analyzer (TGA), using the specific temperature program shown in Figure 3-15. The analysis was done under vacuum conditions (1 mm Hg).
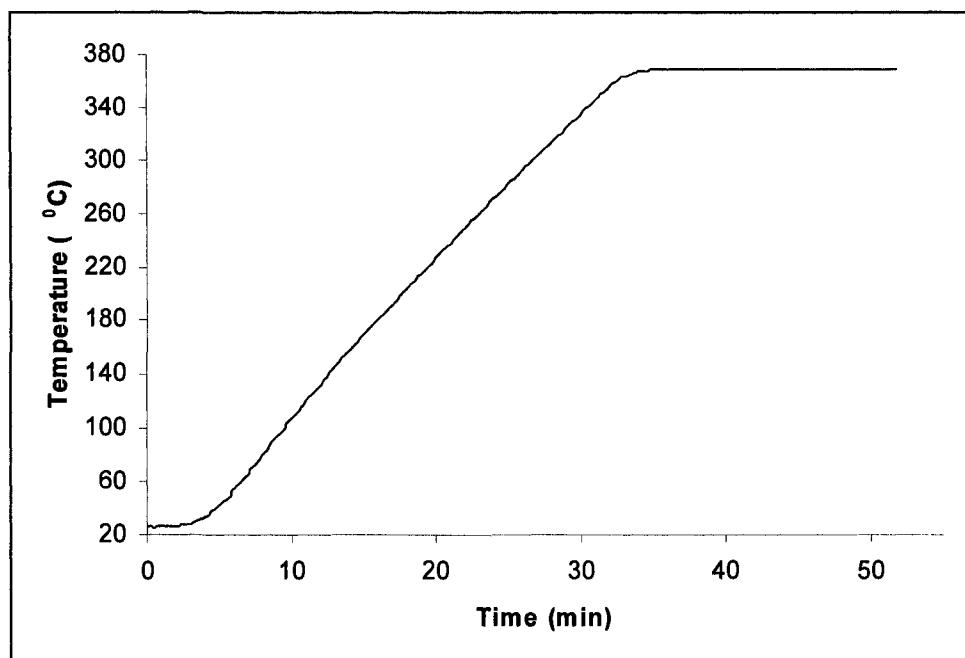
Figure 3-15 TGA temperature program

The vacuum-distillation curves of the recovered liquid hydrocarbon samples are shown in Figures 3-16 to 3-22. Each figure includes recovered liquid hydrocarbon from pentane-, hexane- and toluene- extracted oilsands that were cracked with the same catalyst. TGA analysis indicates that pentane and hexane extract lighter hydrocarbon fractions and smaller amounts of residuum from oilsands samples than toluene.

When raw oilsands bitumen, was extracted by different solvents,increasing extraction of residuum was observed with increasing alkane chain length of the solvents (shown in Figure 3-16). For pentane extracted bitumen, the residual masse reduced to 22 wt% from the initial mass after heating in a vacuum to 350°C. Hexane can extract heavier compoents than pentane, but much less than toluene. There was 33 wt% residuum remaining in hexane-extracted bitumen. For toluene-extracted bitumen, the residual mass

reduced to 44 wt%, indicating that pentane or hexane extraction of bitumen from raw oilsands significantly reduces the extraction of heavy components.
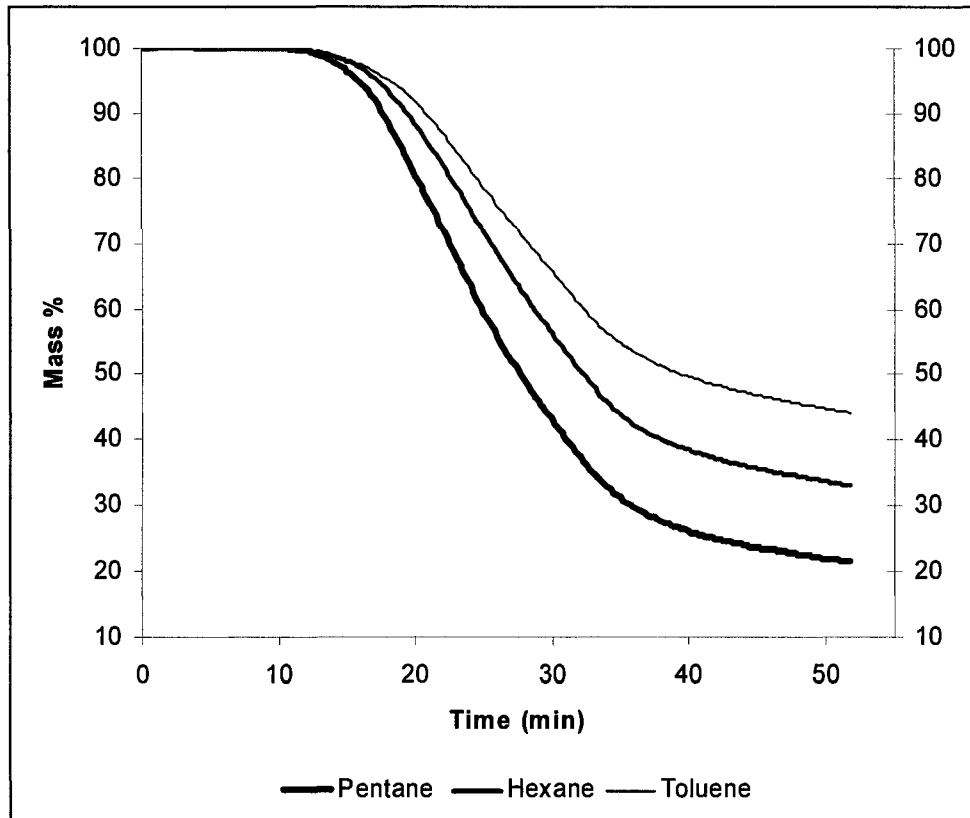


Figure 3-16 Vacuum-distillation curves of bitumen extracted by pentane, hexane and toluene from raw oilsands

Increased residual mass of liquid hydrocarbon extracted by different solvents (pentane, hexane and toluene) from thermally cracked oilsands are shown in Figure 3-17. After pentane or hexane extraction, the liquid hydrocarbon residual mass reduced to 25 wt% from their respective initial masses. For liquid hydrocarbon extracted by toluene, the residual mass reduced to 28 wt%, which indicates that thermal cracking breaks down some residuum in the raw bitumen into lighter components. For thermally cracked

oilsands, toluene extracted liquid hydrocarbon has 3% higher residual mass than hexane or pentane extracted samples.



Figure 3-17 Vacuum-distillation curves of liquid hydrocarbon samples extracted by pentane, hexane and toluene from thermally cracked oilsands

For zeolite Y-cracked oilsands, residual masses in liquid hydrocarbon samples extracted by pentane, hexane and toluene are shown in Figure 3-18. For liquid hydrocarbon extracted by pentane, the residual mass reduced to 22 wt% from the initial masses. For liquid hydrocarbon extracted by hexanes or toluene, the residual masses reduced to 24 wt% and 29 wt% from their respective initial masses. The residual mass of

liquid hydrocarbon extracted by toluene was 5 to 7% higher than the mass of liquid

hydrocarbon extracted by hexanes and pentane.



Figure 3-18 Vacuum-distillation curves of liquid hydrocarbon samples extracted by pentane, hexane and toluene from zeolite Y cracked oilsands

For sodium chabazite cracked oil sands, residual masses of liquid hydrocarbon

samples extracted by different solvents (pentane, hexanes and toluene) are shown in

Figure 3-19. After pentane extraction, the residual mass of liquid hydrocarbon reduced to

24 wt% from the initial masses. For liquid hydrocarbon samples extracted by hexane and

toluene, the residual masses reduced to 22 wt% and 27 wt% from their respective initial

masses. Toluene extracted liquid hydrocarbon residual mass was 3 to 5% higher than that

of pentane and hexane extracted.
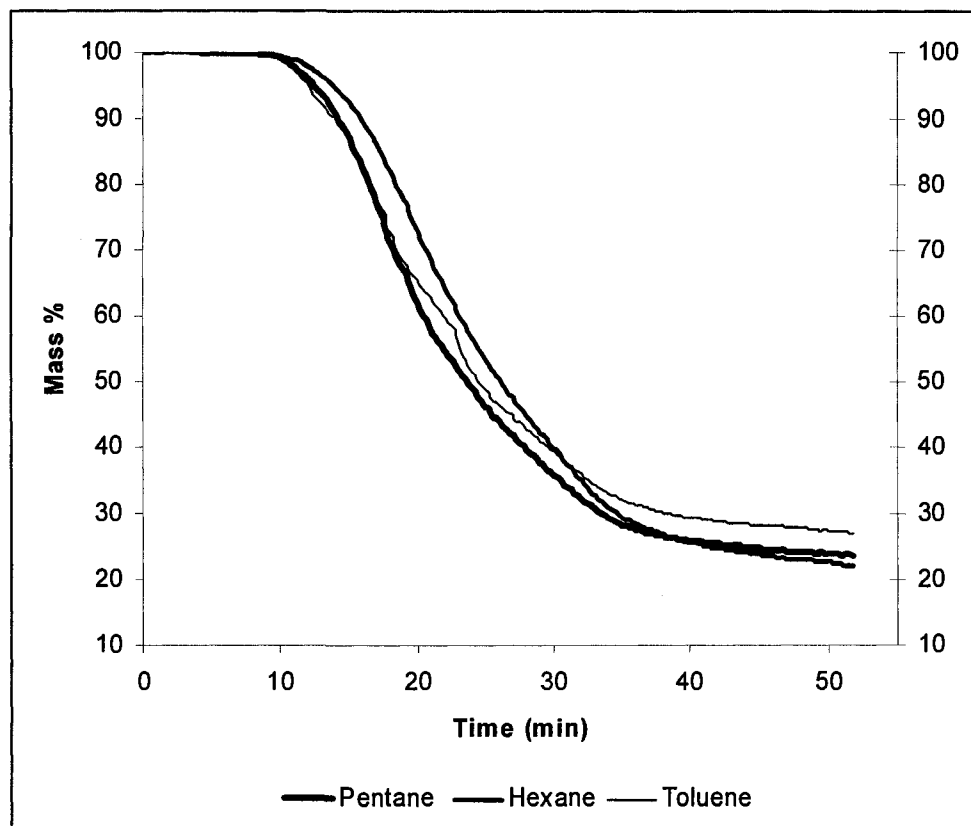


Figure 3-19 Vacuum-distillation curves of liquid hydrocarbon samples extracted by
pentane, hexane and toluene from Na-chabazite cracked oilsands

For calcium chabazite cracked oilsands, residual masses of liquid hydrocarbon

extracted by different solvents (pentane, hexanes and toluene) is shown in Figure 3-20.

After pentane extraction, the residual mass of the liquid hydrocarbon sample reduced to

22 wt% from the initial masses. For liquid hydrocarbon extracted by hexane and toluene,

the residual masses reduced to 20 wt% and 24 wt% from their respective initial masses.

The toluene extracted liquid hydrocarbon sample has a residual mass 2 to 4% higher than

of pentane and hexane extracted.
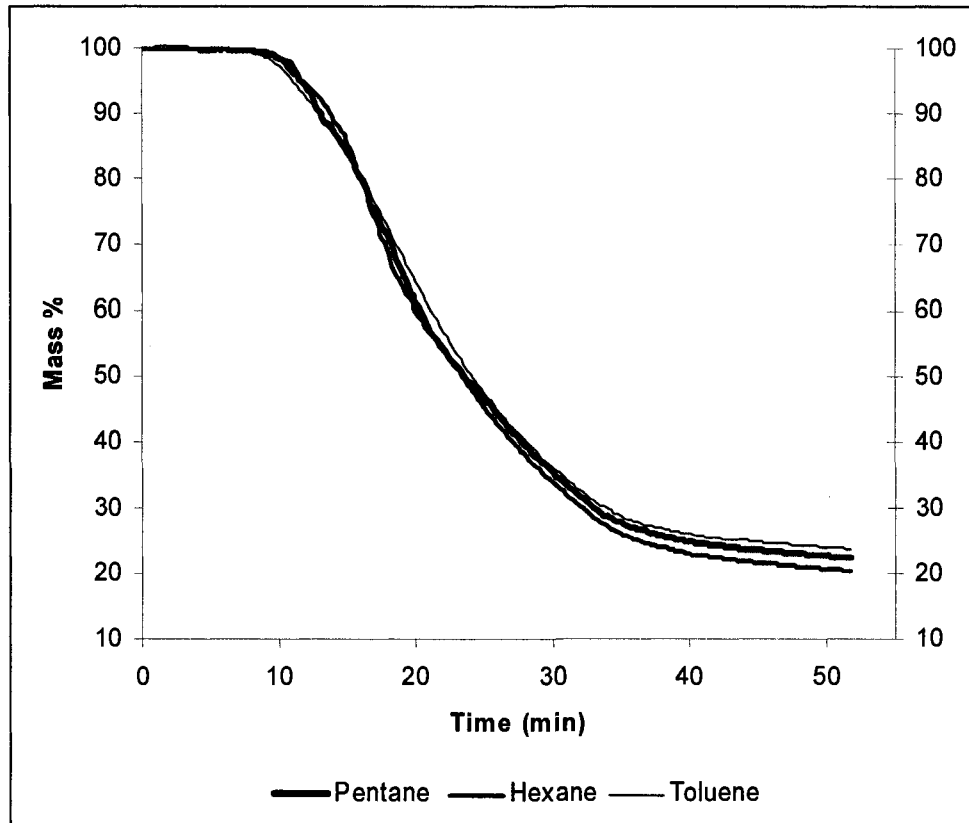


Figure 3-20 Vacuum-distillation curves of liquid hydrocarbon samples extracted by
pentane, hexane and toluene from Ca-chabazite cracked oilsands

For clinoptilolite (New Mexico) cracked oilsands, residual masses of liquid

hydrocarbon extracted by different solvents (pentane, hexanes and toluene) is shown in

Figure 3-21. The residual mass of liquid hydrocarbon extracted by pentane reduced to 18

wt% from the initial masses. For hexane and toluene-extracted liquid hydrocarbon, the

residual masses reduced to 21 wt% and 24 wt% from their respective initial masses.

Toluene extracted liquid hydrocarbon has a 3 to 6% higher residual mass than hexanes and pentane extracted.
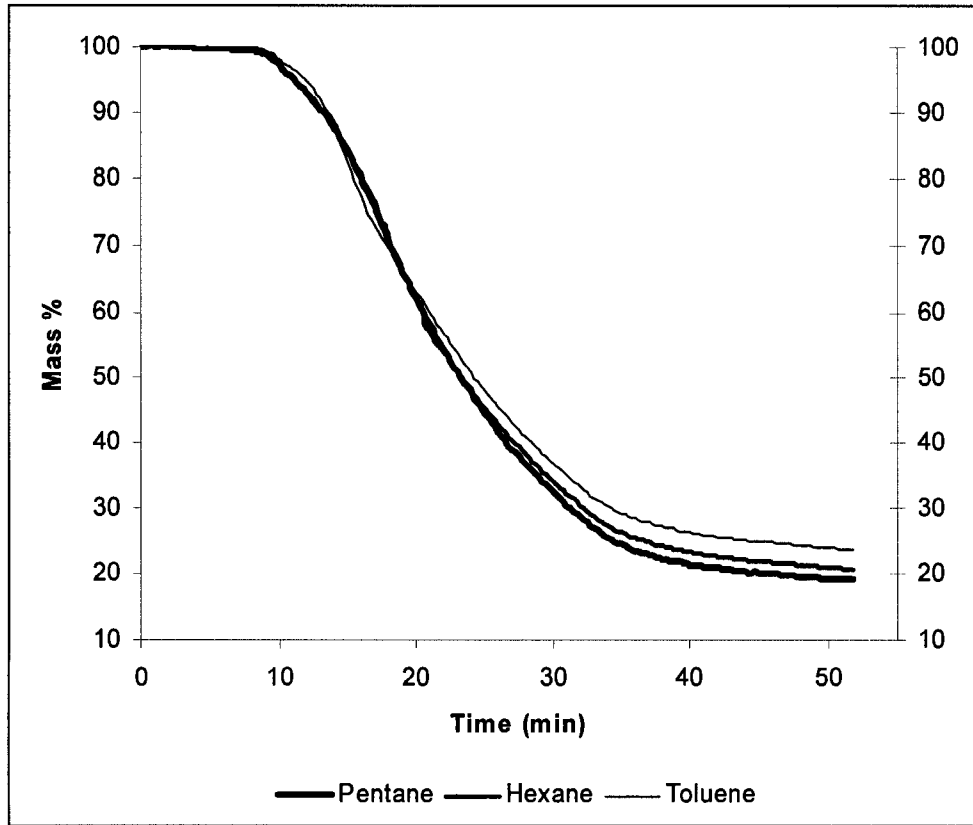


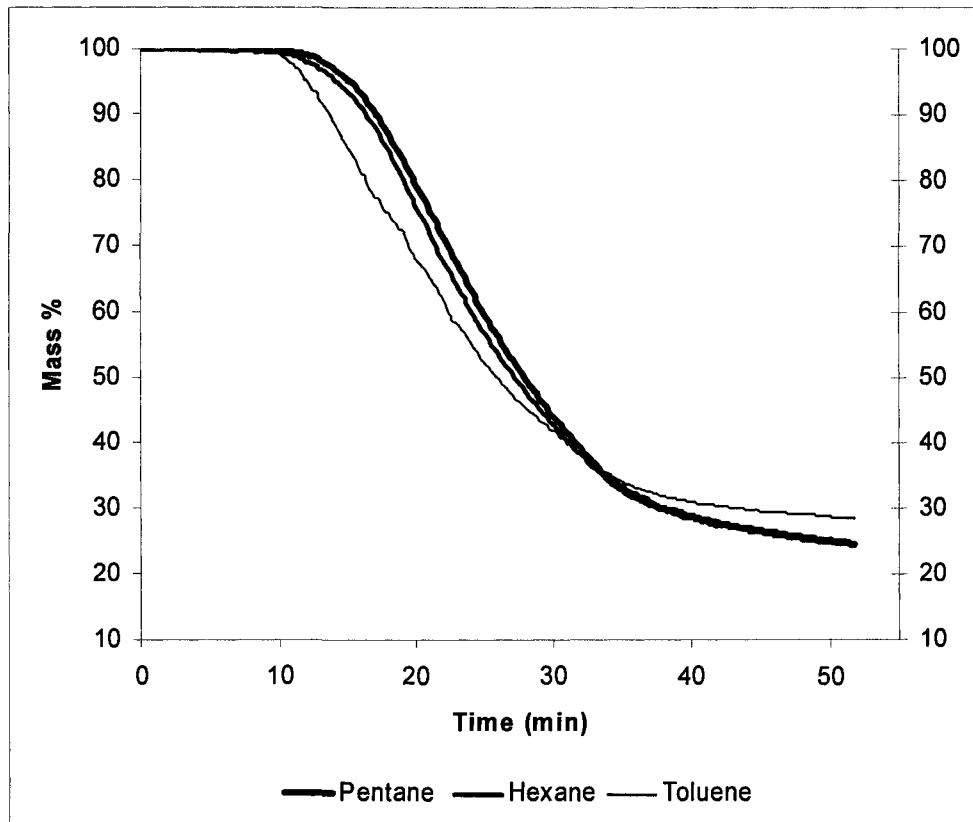Figure 3-21 Vacuum-distillation curves of liquid hydrocarbon samples extracted by pentane, hexane and toluene from clinoptilolite (New Mexico) cracked oilsands

For clinoptilolite (Australia) cracked oilsands, an increase in residual mass was observed (shown in Figure 3-22) in liquid hydrocarbon samples extracted by pentane, hexane and toluene. The residual mass of the liquid hydrocarbon sample extracted by pentane reduced to 12 wt% from the initial masses, which is the lowest residuum observed in all of the recovered liquid hydrocarbon samples. For liquid hydrocarbon samples extracted by hexane and toluene, the residual masses reduced to 16 wt% and 22

wt% from their respective initial masses, which is also lower than for any other liquid

hydrocarbon sample extracted by hexane and toluene. The residual mass of the toluene

extracted liquid hydrocarbon sample was 6 to 10% higher than hexane and pentane-

extracted samples. As shown by vacuum distillation curves, the clinoptilolite (Australia)-
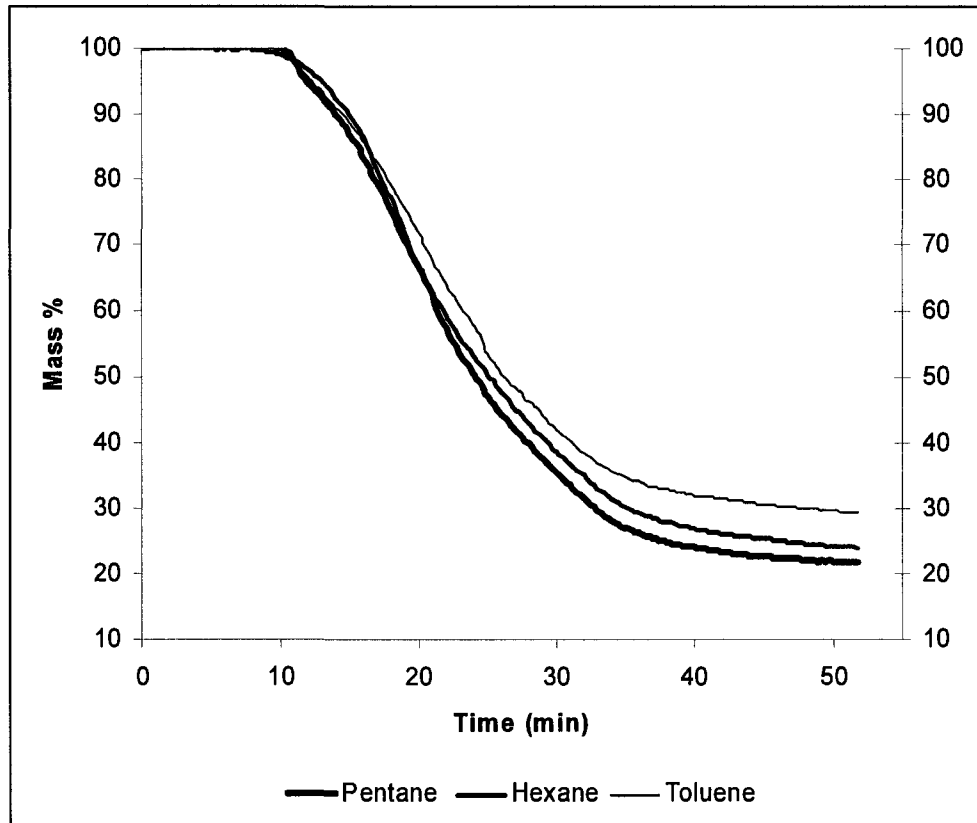
cracked oilsands yield liquid hydrocarbon sample has the lowest residual content.
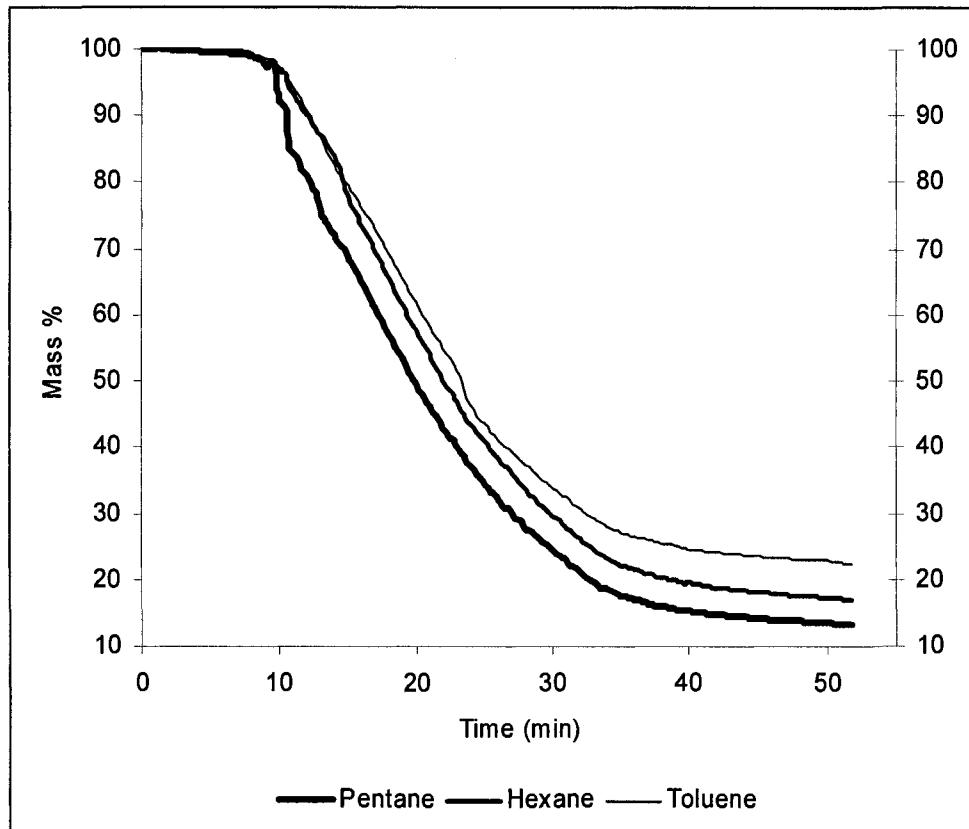


Figure 3-22 Vacuum-distillation curves of liquid hydrocarbon samples extracted by
pentane, hexane and toluene from clinoptilolite (Australia) cracked oilsands

Combining all individual vacuum distillation curves together, raw oilsands

extracted by toluene reduced to a mass of 44% after vacuum distillation; when pentane or

hexane was used, the residual masses were much lower (22% or 33% respectively). In

contrast, sodium chabazite cracked liquid hydrocarbon produces 24%, 22%, 27% (22%,

20%, 24% with calcium chabazite) residual masses from pentane, hexane and toluene extracts respectively, which is lower than that of raw, thermal and zeolite Y cracked samples. Liquid hydrocarbon extracted from clinoptilolite (Australia)-cracked samples produces 12%, 16% and 22% residual masses from pentane, hexane and toluene extracts respectively, which are significantly lower than for raw, thermally cracked or zeolite Y-cracked samples. Cracking with clinoptilolite from New Mexico gives similar results: 18%, 21% and 24% residual masses from pentane, hexane and toluene extraction.

Vacuum distillation curves of recovered liquid hydrocarbon samples extracted by the same solvent are shown in Figures 3-23 to 3- 25. Natural clinoptilolite catalysts crack the bitumen into lighter components than thermal cracking or catalytic cracking with other agents, including commercial zeolite Y, sodium chabazite and calcium chabazite. This trend is consistent for the bitumen using pentane, hexane or toluene as the solvent.

Pentane-extracted liquid hydrocarbon samples from oilsands cracked with clinoptilolites from Australia and New Mexico are reduced to 12 wt% and 18 wt% of their respective initial masses after being heated in a vacuum to 350°C. In comparison, extracts from raw and thermally cracked oilsands have residual masses of 22 wt% and 25 wt%. The residual masses from the natural clinoptilolite samples are approximately 4 to 10% lower than those generated by cracking with zeolite Y, and 6 to 11% lower than the calcium and sodium chabazite samples; this indicates that the liquid hydrocarbon samples generated using clinoptilolite catalysts contain the lightest hydrocarbon fractions.
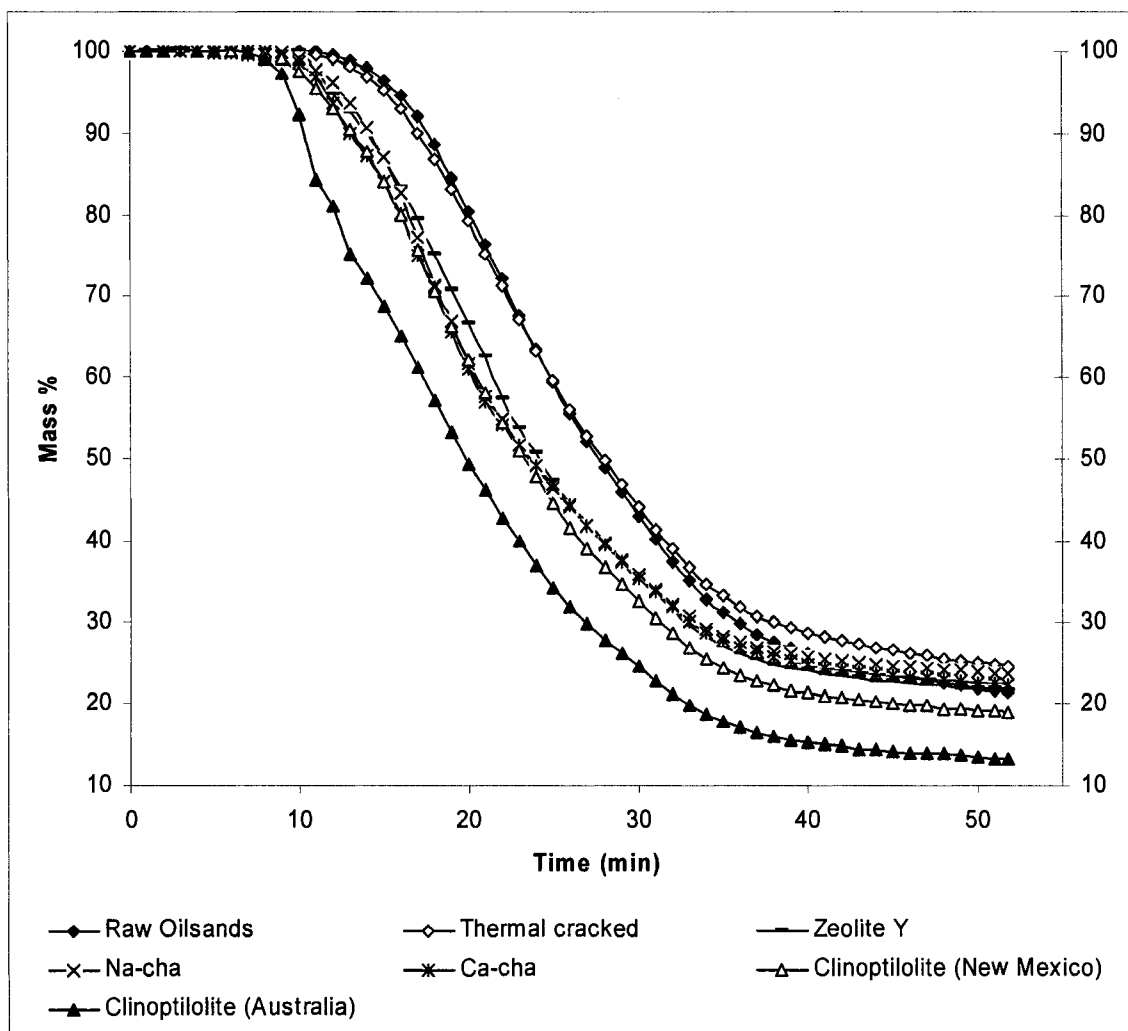
Figure 3-23 Vacuum-distillation curves of liquid hydrocarbon samples extracted by pentane from raw and cracked oilsands

When the raw and cracked samples are extracted with hexane instead of pentane, increased residual masses are observed (Figure 3-24), indicating that hexane extracts heavier hydrocarbon fractions. After hexane extraction, we observe residual masses of 33 wt% and 25 wt% for raw and thermally cracked liquid hydrocarbon. 22 wt% and 21 wt% for calcium and sodium chabazite cracked liquid hydrocarbon. Consistent with the results from pentane extraction, the lowest residual mass (16%) is observed for samples cracked with Australian clinoptilolite.
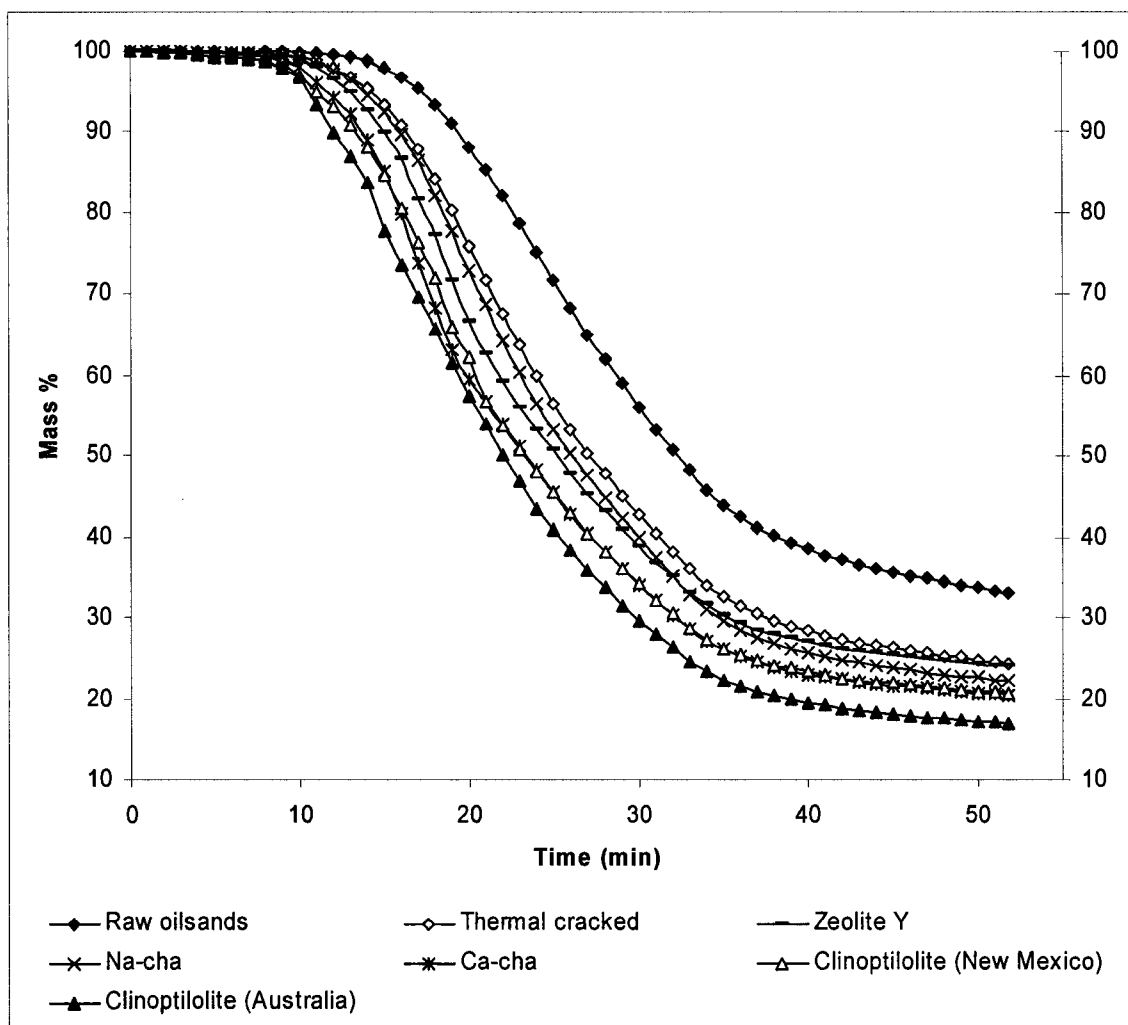
Figure 3-24 Vacuum-distillation curves of liquid hydrocarbon samples extracted by hexane from raw and cracked oilsands

When the raw bitumen is cracked with clinoptilolites and extracted by lighter hydrocarbons, the residuum content decreases by only 4-9 wt%, compared to the analogous toluene-extracted samples, indicating that few asphaltenes remain after the cracking reactions. In contrast, pentane and hexane extraction of raw oilsands reduces the residuum content by 13-23 wt%, compared to toluene extraction, indicating that a significant portion of the asphaltene content of raw oilsands is not extracted using the lighter hydrocarbons.

Asphaltenes are soluble in toluene and insoluble in lighter n-alkane hydrocarbons.[10] The cracked samples were extracted with toluene; increased residual masses were observed (Figure 3-25). After toluene extraction, residual masses of raw bitumen reduced to 44 wt% from their respective initial masses. For thermally and zeolite Y cracked oilsands yield bitumen, the residual masses reduced to 28 wt% and 29 wt%. The lowest residual mass (22%) is observed for samples cracked with Australian clinoptilolite. This result indicates that approximately 50% of the asphaltenes in raw bitumen samples were broken down into smaller molecules after cracking with the Australia-clinoptilolite catalyst.
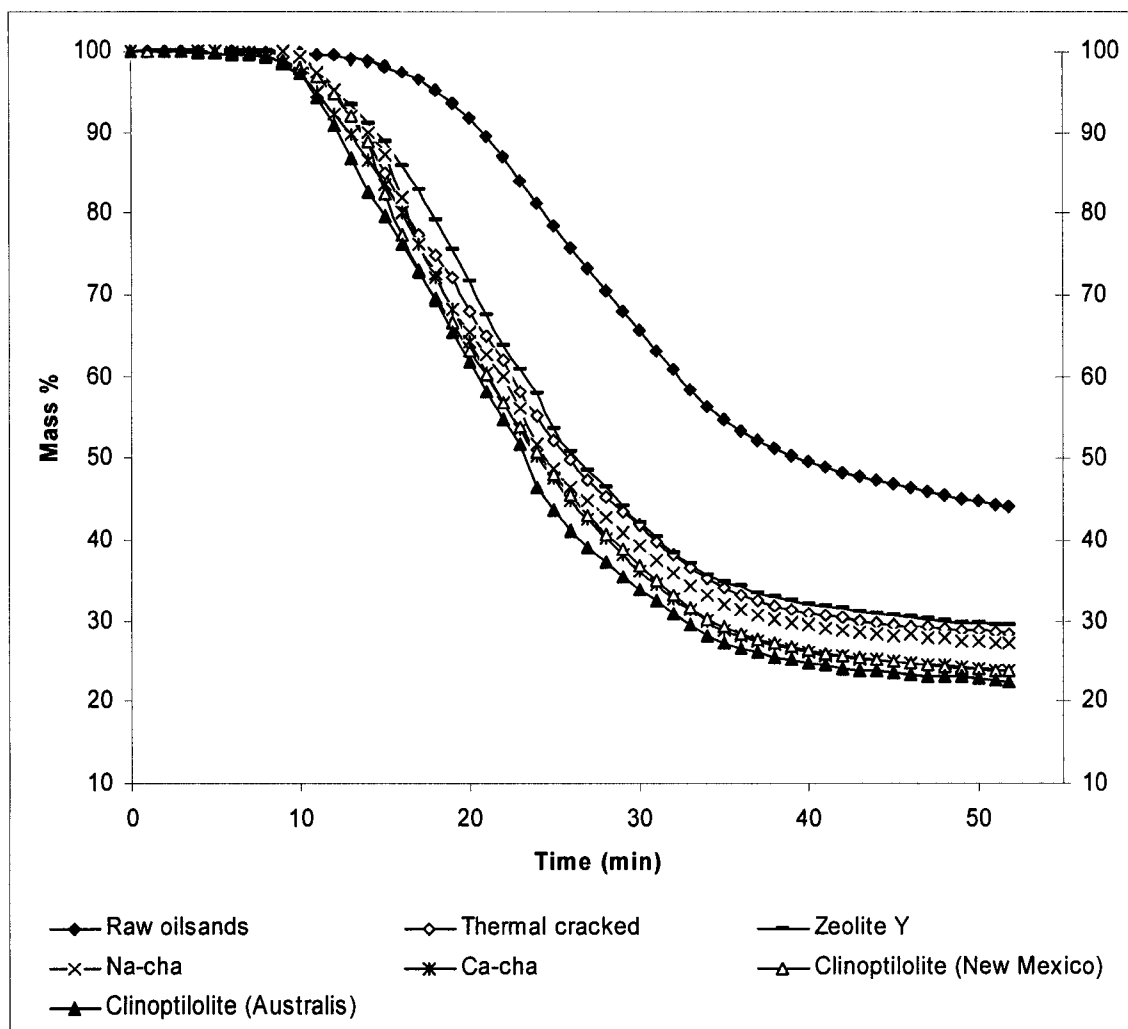
Figure 3-25 Vacuum-distillation curves of liquid hydrocarbon extracted by toluene from raw and cracked oilsands

The vacuum distillation data were converted from vacuum pressure to absolute pressure by using ASTM D1160 Temperature–Pressure Conversion Table for petroleum hydrocarbons (shown in Figure 3-26). [11]
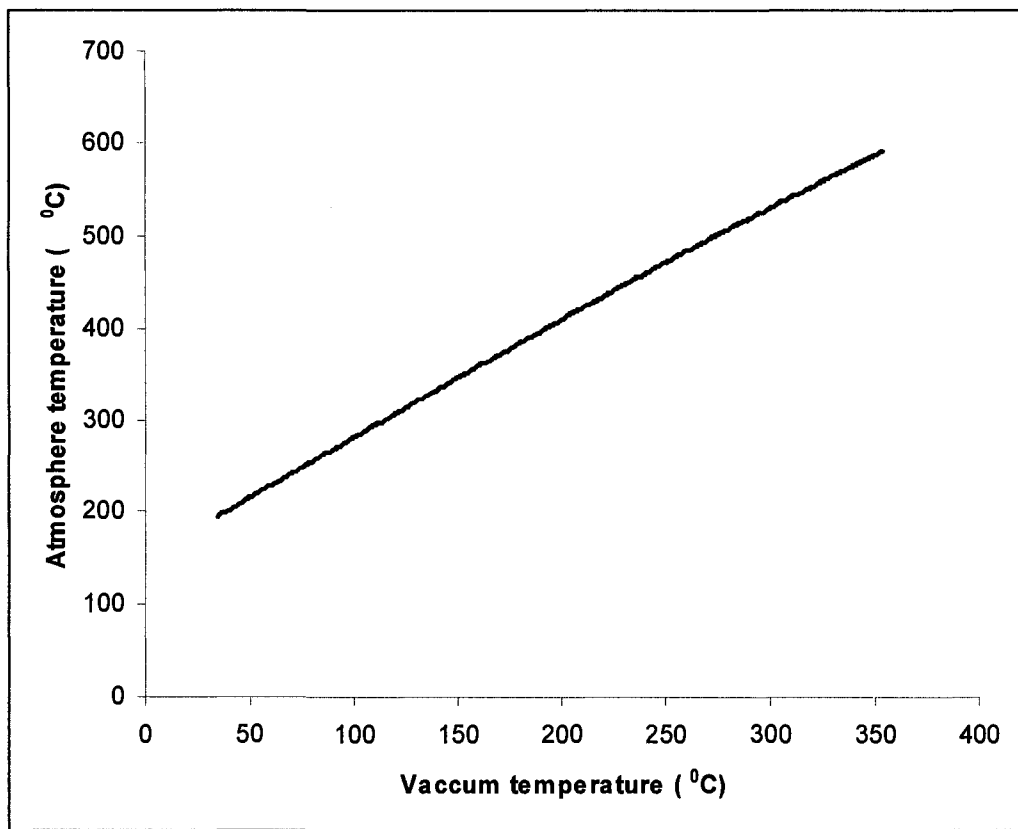
Figure 3-26 ASTM D1160 Temperature–Pressure Conversion Table (from 1mm Hg –
760 mm Hg Absolute Pressure)

When the vacuum distillation curves of the liquid hydrocarbon samples are converted to atmospheric pressure values in order to approximate standard petroleum fractions, it is observed that the natural zeolite-cracked products are distributed into much lighter components than raw, thermally-cracked, or zeolite Y-cracked samples (Tables 3-9 to 3-11).

In toluene extracts, the raw oilsands sample has the highest residuum content (65.9 wt%), thermal and zeolite Y cracked bitumen have 42.0 wt% and 42.6 wt% of residuum, respectively. After using natural chabazite cracking as a catalyst, the residuum of removed liquid hydrocarbons reduces to 39.7 wt% and 36.7 wt%. The clinoptilolite-catalyzed samples have the lowest (37.2 and 34.3 wt%) residuum. The reduced residuum

content of the clinoptilolite cracked samples corresponds to increases in the lighter

naphtha, kerosene and gas oil fractions (Table 3-9).

Table 3-9 Absolute pressure boiling point distribution of liquid hydrocarbon samples extracted by toluene (converted from data for vacuum condition by ASTM D1160)

| Liquid hydrocarbon samples | Naphtha | Kerosene | Distillate fuel oil | Gas oil or lube stock | Residuum |
|---|---|---|---|---|---|
| Temperature | (<191°C) | (191°C - 277°C) | (277°C - 343°C | (343°C - 566°C) | (>566°C) |
| Raw oilsands | - | 0.2 | 0.6 | 33.3 | 65.9 |
| Thermal cracking | - | 0.5 | 8.0 | 49.5 | 42.0 |
| Zeolite Y | - | 0.4 | 6.5 | 50.5 | 42.6 |
| Na-chabazite | - | 0.1 | 8.1 | 52.1 | 39.7 |
| Ca-chabazite | - | 1.5 | 9.4 | 52.4 | 36.7 |
| Clinoptilolite (New Mexico) | 0.2 | 1.1 | 7.3 | 54.2 | 37.2 |
| Clinoptilolite (Australia) | - | 1.6 | 12.7 | 51.4 | 34.3 |

A higher proportion of lighter fractions is also observed in the pentane- and

hexane-extracted, natural zeolite-cracked samples than in the corresponding raw,

thermally cracked or zeolite Y-cracked oilsands (Table 3-10 and 3-11). Of the pentane

extracts, the raw oilsands sample and thermally cracked oilsands sample have the highest

residuum content (43.3 and 44.9 wt%) while zeolite Y-cracked bitumen has a 35.8 wt%

residuum. Using the natural chabazite cracking catalyst, the residuum of recovered liquid

hydrocarbon reduces to 36.2 wt% and 35.9 wt%, respectively. The clinoptilolite-

catalyzed samples have the lowest (33.0 wt%, 25.1 wt%) residuum. The reduced

residuum content of the clinoptilolite samples corresponds to increases in the lighter

naphtha, kerosene and gas oil fractions (Table 3-10). There was about 22 wt% distillate fuel oil in clinoptilolite (Australia) treated and pentane extracted liquid hydrocarbon, which is 20% more than in the raw oilsands bitumen.

Table 3-10 Absolute pressure boiling point distribution of liquid hydrocarbon samples extracted by pentane (converted from vacuum condition by ASTM D1160)

| Liquid hydrocarbon samples | Naphtha | Kerosene | Distillate fuel oil | Gas oil or lube stock | Residuum |
|---|---|---|---|---|---|
| Temperature | (<191°C) | (191°C - 277°C) | (277°C - 343°C | (343°C - 566°C) | (>566°C) |
| Raw oilsands | - | - | 1.3 | 55.4 | 43.3 |
| Thermal cracking | - | 0.1 | 1.7 | 53.2 | 44.9 |
| Zeolite Y | - | - | 8.0 | 56.2 | 35.8 |
| Na-chabazite | - | 0.4 | 6.5 | 56.9 | 36.2 |
| Ca-chabazite | 0.2 | 0.7 | 9.8 | 53.4 | 35.9 |
| Clinoptilolite (New Mexico) | - | 1.1 | 8.9 | 57.0 | 33.0 |
| Clinoptilolite (Australia) | - | 2.6 | 22.0 | 50.3 | 25.1 |

With hexanes as the solvents, the raw oilsands sample has the highest residuum content (56.3 wt%), while thermal and zeolite Y cracked bitumen have 43.0 wt% and 39.1 wt% residuum. In natural chabazite cracked oilsands, the residuum of the liquid hydrocarbon samples reduces to 40 wt% and 34.5 wt% for Na-chabazite and Ca-chabazite respectively. The clinoptilolite-catalyzed samples, especially Australian samples (30.0 wt%), have the lowest residuum. The reduced residuum content of the clinoptilolite samples corresponds to increases in the amounts of the lighter naphtha, kerosene and gas oil fractions (Table 3-11).

Table 3-11 Absolute pressure boiling point distribution of liquid hydrocarbon samples extracted by hexanes (converted from data for vacuum condition by ASTM D1160)

| Liquid hydrocarbon samples | Naphtha | Kerosene | Distillate fuel oil | Gas oil or lube stock | Residuum |
|---|---|---|---|---|---|
| Temperature | (<191°C) | (191°C - 277°C) | (277°C - 343°C | (343°C - 566°C) | (>566°C) |
| Raw oilsands | - | 0.1 | 0.7 | 42.9 | 56.3 |
| Thermal cracking | - | 0.5 | 2.8 | 53.7 | 43.0 |
| Zeolite Y | 0.1 | 0.4 | 4.9 | 55.5 | 39.1 |
| Na-chabazite | 0.2 | 0.4 | 3.2 | 56.2 | 40 |
| Ca-chabazite | 0.1 | 0.9 | 7.2 | 57.3 | 34.5 |
| Clinoptilolite (New Mexico) | 0.2 | 1.1 | 7.3 | 54.2 | 37.2 |
| Clinoptilolite (Australia) | 0.4 | 1.7 | 11.3 | 56.6 | 30.0 |

Comparison of vacuum distillation curves and recovery from oilsands samples establishes that natural clinoptilolites break down the heavier hydrocarbons (like asphaltenes) in bitumen into much lighter components than simple thermal cracking or commercial zeolite Y-catalyzed cracking. Light hydrocarbons, such as pentane or hexane, can selectively extract the commercially valuable fractions from the clinoptilolite-cracked samples, leaving the few remaining asphaltenes and other undesirable heavier components in the exhausted sands. This results in the production of lighter, less viscous, and therefore more transportable, petroleum fractions that contain a higher proportion of fuel-grade hydrocarbons.

**3.2.3 The recovered liquid hydrocarbon H/C ratio**

The carbon and hydrogen concentration of the recovered liquid hydrocarbon samples was detected on a Carlo Erba EA1108 CHNS-O elemental analyzer. For oilsands treated with different cracking agents, a decreased H/C ratio of liquid hydrocarbon samples extracted by different solvents (pentane, hexane and toluene) was observed (shown in Table 3-12), indicating that light solvents such as pentane and hexane extract lighter fractions than toluene.

Since toluene can co-extract the asphaltene molecules, toluene-extracted liquid hydrocarbon samples have the lowest H/C ratio (1.401-1.495) while pentane extracted liquid hydrocarbon samples have the highest H/C ratio (1.476-1.599). Compared with the H/C ratio (~1.22) of hot water extracted Athabasca bitumen, the liquid hydrocarbon samples extracted from natural zeolite cracked oilsands have a much higher H/C ratio (1.40~1.60).[2]

Table 3-12 H/C ratio of liquid hydrocarbon extracted by pentane, hexane and toluene from raw and cracked oilsands

| Liquid hydrocarbon samples | H/C ratio | | |
|---|---|---|---|
| | Pentane extracted | Hexane extracted | Toluene extracted |
| Raw oilsands | 1.599 | 1.468 | 1.495 |
| Thermal cracking | 1.476 | 1.471 | 1.416 |
| Zeolite Y | 1.479 | 1.465 | 1.436 |
| Na-chabazite | 1.482 | 1.484 | 1.444 |
| Ca-chabazite | 1.479 | 1.452 | 1.441 |
| Clinoptilolite (New Mexico) | 1.482 | 1.481 | 1.423 |
| Clinoptilolite (Australia) | 1.476 | 1.462 | 1.401 |

### 3.2.4 Removal of contaminants

3.2.4.1 Nitrogen content reduction

The nitrogen content in the liquid hydrocarbon samples was detected using a CHNS-O elemental analyzer. The total nitrogen in 12 g of raw oilsands extracted by toluene was assumed to be 100 wt%. Table 3-13 shows the percentage of nitrogen removed from raw and cracked oilsands liquid hydrocarbon samples extracted by toluene. An increase in nitrogen removal was observed in zeolite cracked samples.

As shown in Table 3-13, thermal cracking removed 11 wt% of nitrogen and zeolite Y cracking removed 14 wt% nitrogen. Sodium chabazite cracking removed 20 wt% of nitrogen and natural clinoptilolites cracking removed 22 and 24 wt% of nitrogen. These results indicate that, after cracking with natural clinoptilolite, more nitrogen was removed from bitumen than after thermal cracking or zeolite Y catalyst cracking.

Table 3-13 Nitrogen removal for liquid hydrocarbon samples from raw and cracked oilsands extracted by toluene

| Liquid hydrocarbon sample | Toluene extracted (wt %) |
|---|---|
| Raw oilsands | 0 |
| Thermal cracking | 11 |
| Zeolite Y | 14 |
| Na-chabazite | 20 |
| Ca-chabazite | 0 |
| Clinoptilolite (New Mexico) | 24 |
| Clinoptilolite (Australia) | 22 |

3.2.4.2 Sulfur content reduction

The sulfur content in liquid hydrocarbon samples was measured using a CHNS-O elemental analyzer. The total sulfur in 12 g of raw oilsands extracted by toluene was assumed to be 100 wt%. Table 3-14 shows the sulfur removed from raw and cracked oilsands liquid hydrocarbon samples extracted by toluene. Increased sulfur removal was observed in zeolite cracked and thermally cracked samples..

As shown in Table 3-14, thermal cracking removed 32 wt% of sulfur. Zeolite Y cracking removed 16 wt% of sulfur. Sodium and calcium chabazite cracking removed 19 wt% and 6 wt% of sulfur. Natural clinoptilolites cracking removed 24~27 wt% of sulfur. This result illustrates that natural clinoptilolites cracking removes more sulfur than cracking with zeolite Y and natural chabazite.

Table 3-14 Sulfur removal for liquid hydrocarbon samples from raw and cracked oilsands extracted by toluene

| Liquid hydrocarbon sample | Toluene extracted (wt %) |
|---|---|
| Raw oilsands | 0 |
| Thermal cracking | 32 |
| Zeolite Y | 16 |
| Na-chabazite | 19 |
| Ca-chabazite | 6 |
| Clinoptilolite (New Mexico) | 24 |
| Clinoptilolite (Australia) | 27 |

3.2.4.3 Vanadium removal

The vanadium concentration in recovered liquid hydrocarbon samples was measured with a Perkin Elmer 6000 quadrupole ICP-MS instrument. Table 3-15 shows

the percentage of vanadium removed from raw and cracked oilsands liquid hydrocarbon samples extracted by different solvents (pentane, hexane and toluene). The natural clinoptilolite sample from New Mexico removes the highest amount of vanadium after the cracking.

After toluene extraction, the vanadium concentration in raw bitumen is 201 ppm. Pentane and hexanes extractions remove 72% and 59% of the vanadium from raw bitumen respectively. This result indicates that vanadium is located mainly in the heavy fractions of bitumen. Compared with the raw bitumen, the vanadium concentration of the thermally cracked liquid hydrocarbon sample is reduced to 64%, indicating that 36% of the vanadium was left in the exhaust sands after toluene extraction. Using pentane and hexane extraction, vanadium in recovered liquid hydrocarbon was removed by 80% and 67% respectively. Zeolite Y cracking removed 28% of the vanadium after toluene extraction while pentane and hexane extraction removed 72% and 63% of the vanadium respectively.

Compared with the raw bitumen, sodium chabazite and calcium chabazite cracking removed 35% and 34% of the vanadium after toluene extraction respectively. Using pentane and hexane extraction, vanadium 79% and 77% was removed, respectively (80% and 74% with calcium chabazite).

The highest vanadium removal was obtained with clinoptilolite (New Mexico) cracked oilsands. About 59% of vanadium was left in the exhausted sands after toluene extraction. Using pentane and hexane extraction, 75% and 67% of the vanadium in liquid hydrocarbon samples was removed. Clinoptilolite (Australia) cracking also removes 33% of vanadium to the exhausted sands after toluene extraction. Using pentane and hexane

extracted bitumen, vanadium in recovered liquid hydrocarbon samples was reduced by 79% and 66% respectively.

Table 3-15 Vanadium removal for different solvents (pentane, hexane and toluene) extracted liquid hydrocarbon from raw and cracked oilsands

| Liquid hydrocarbon samples | Vanadium removal (%) | | |
|---|---|---|---|
| | Extracted by Pentane | Extracted by Hexane | Extracted by Toluene |
| Raw oilsands | 72 | 59 | 0 |
| Thermal cracking | 80 | 67 | 36 |
| Zeolite Y | 72 | 63 | 28 |
| Na-chabazite | 79 | 77 | 35 |
| Ca-chabazite | 80 | 74 | 34 |
| Clinoptilolite (New Mexico) | 75 | 67 | 59 |
| Clinoptilolite (Australia) | 79 | 66 | 33 |

3.3.4.4 Nickel removal

The nickel concentration in recovered liquid hydrocarbon samples was also measured with a Perkin Elmer 6000 quadrupole ICP-MS instrument. Table 3-16 shows the nickel removed from raw and cracked oilsands liquid hydrocarbon samples extracted by different solvents (pentane, hexane and toluene). The natural clinoptilolite sample from Australia removes the most nickel after the cracking.

After toluene extraction, the nickel concentration in raw bitumen is 100 ppm. Pentane and hexane extractions remove 29% and 9% of the nickel in raw bitumen, respectively. This result indicates that nickel is located mainly in the light fraction of

73

bitumen. Compared with the raw bitumen, the nickel concentration of the thermal cracking yield liquid hydrocarbon sample was reduced by 77%, indicating that 23% of nickel was left in exhausted sands after toluene extraction. Using pentane and hexanes extraction, the nickel in recovered liquid hydrocarbon samples was reduced by 52% and 42%, respectively. Zeolite Y cracking removes 15% of the nickel after toluene extraction, while pentane and hexane extractions removed 35% and 21% respectively.

Compared with the raw bitumen, sodium chabazite and calcium chabazite cracking removed 9% and 16% of nickel after toluene extraction respectively. Using pentane and hexane extraction, nickel was removed by 44% and 40%, respectively (44% and 37% with calcium chabazite).

The highest nickel removal was obtained with clinoptilolite (Australia) cracked oilsands. About 31% of nickel was left in the exhausted sands after toluene extraction. Using pentane and hexanes extractions, the nickel in recovered liquid hydrocarbon was reduced by 52% and 34%, respectively. Clinoptilolite (New Mexico) cracking removed 3% of nickel after toluene extraction while pentane and hexane extraction both removed 42% of nickel.

Table 3-16 Nickel removal for different solvents (pentane, hexane and toluene) extracted liquid hydrocarbon from raw and cracked oilsands

| Samples | Nickel removal (%) | | |
| --- | --- | --- | --- |
| | Extracted by Pentane | Extracted by Hexane | Extracted by Toluene |
| Raw oilsands | 29 | 9 | 0 |
| Thermal cracking | 52 | 42 | 23 |
| Zeolite Y | 35 | 21 | 15 |
| Na-chabazite | 44 | 40 | 9 |
| Ca-chabazite | 44 | 37 | 16 |
| Clinoptilolite (New Mexico) | 42 | 42 | 3 |
| Clinoptilolite (Australia) | 52 | 34 | 31 |

[1] S M. Kuznicki, W C. McCaffrey, J Bian, Nature Zeolite bitumen cracking and upgrading, *Microporous and Mesoporous Materials*, Vol.105, pp. 268-272. (2007).

[2] S Zhao, L S. Kotlyar, Solid contents, properties and molecular structure of asphaltenes from different oils ands, *Fuel*, Vol. 80, pp. 1907-1914. (2001)

[3] G. Tonetto, J. Atias, H. de Lasa, FCC catalysts with different zeolite crystallite sizes: acidity, structure properties and reactivity, *Applied Catalysis A*: General 270, pp. 9-25. (2004)

[4] D W. Breck, Zeolite Molecular Sieves structure, chemistry, and use, *Juhn wiley & Sons*, New York. pp. 177.

[5] Ch. Baerlocher, L. B. McCusker, Database of zeolite structure: http://www.iza-structure.org/databases/

[6] T J. Grey, D Nicholson, J D. Gale, B K. Peterson, A simulation study of the adsorption of nitrogen in Ca-chabazite, *Applied Surface Science*, Vol. 196, pp. 105-114. (2002)

[7] D W. Breck, Zeolite Molecular Sieves structure, chemistry, and use, *John Wiley & Sons*, New York. pp.138.

[8] D W. Breck, Zeolite Molecular Sieves structure, chemistry, and use, *John Wiley & Sons*, New York. pp. 139.

[9] R. Le Van Mao, N. Al-Yassir, L. Lu, New method for the study of surface acidity of zeolites by $NH_3$-TPD, using a PH-meter equipped with an ion selective electrode, *Catalysis Letters*, Vol .112, Nos.1-2. (2006)

[10] K. Akbarzadeh, A. Dhillon, W Y. Svrcek, H W. Yarranton, Methodology for the Characterization and Modeling of Asphaltene Precipitation from Heavy Oils Diluted with *n*-Alkanes, *Energy Fuels*, Vol.18, pp. 1434-1441. (2004)

[11] A. W. Drews. (editor) *ASTM Manual on Hydrocarbon Analysis*, 4th Edition; pp. 244-245.

# CHAPTER 4

# CONCLUSION

## 4.1 Catalysts

Economical, single pass, disposable natural zeolites have several important properties which make them excellent catalysts for the breakdown of oilsands bitumen. One key feature is the platy morphology of both chabazite and clinoptilolite, which results in a large exterior surface area. It is this surface where cracking can occur when asphaltene molecules bind to the catalyst surface.

Natural zeolites chabazite and clinoptilolite also have a highly crystalline structure as observed by XRD. Raw sedimentary chabazite contains impure phases (clinoptilolite and erionite), which can be successfully converted to a chabazite-like structure by dissolving them in an alkaline sodium silicate solution. The upgrading process also removes the contaminants (Mg, S and Cl) in raw sedimentary chabazite. After calcination, both sodium chabazite and calcium chabazite have a stable dehydrated form. The two clinoptilolite samples from New Mexico and Australia contain different impure phases and clinoptilolite from New Mexico has more impurities as indicated by XRD. After calcination, both clinoptilolites have very stable dehydrated forms.

BET surface area analysis shows that calcium chabazite has a higher total surface area than commercial zeolite Y. The two clinoptilolite samples, however, have lower total surface areas and micropore surface areas, than either zeolite Y or chabazite. The micropore sizes of zeolite Y and calcium chabazite are distributed evenly over a wide

range (from 15 nm to 150 nm). In contrast, the two clinoptilolite samples have very uniform macropores, with size varying in a narrow range (from 15 nm to 20 nm).

The results of elemental analysis show that the natural zeolites calcium chabazite and clinoptilolite have higher Si/Al ratios than zeolite Y. This indicates that chabazite and clinoptilolite have a more stable framework and a greater number of acid sites, which suggest that the catalytic properties of the natural zeolite will be more stable during a high temperature cracking reaction.

Although clinoptilolite samples have lower calculated acid sites, they also have lower total surface areas. This result indicates that clinoptilolite samples have a higher calculated average acid site density, especially the clinoptilolite (Australia), which has the highest average acid site density for all tested catalysts.

As ammonia TPD profiles show that both chabazite and clinoptilolite samples have greater acid strength than zeolite Y. Calcium chabazite and clinoptilolite (New Mexico) have more overall desorption area and more medium desorption area, which indicates that they have more acid strength and a great number of medium acid sites.

Modified chabazite and clinoptilolite have the potential to crack the bitumen in oilsands more efficiently than commercial zeolite Y. These natural zeolites can potentially improve the efficiency of the visbreaking process and enhance the economics of in-field bitumen upgrading. If the catalysts can remove nitrogen, sulfur and heavy metals contaminants, initial product quality of cracked bitumen from the oilsands could be improved dramatically.

## 4.2 Recovered liquid hydrocarbons

As discussed in earlier work, Bowie chabazite is an acidic, highly crystallized catalyst with a large surface area and platy morphology, and these properties contribute to its cracking capacity. Clinoptilolite, which has similar morphology to Bowie chabazite, has a more stable framework and is acidic in nature, which may explain its exceptional performance as a cracking catalyst.

The once-through pentane extraction results show that clinoptilolite, an economic, abundant natural mineral, is an effective cracking catalyst, which can break down the heavy molecules of bitumen within oilsands into lighter fractions more effectively than thermal cracking.

The liquid hydrocarbons recovery from pentane-, hexane- and toluene-extracted raw and cracked oilsands samples show that natural clinoptilolite (New Mexico) cracked oilsands samples have a higher liquid hydrocarbon recovery rate than those obtained with zeolite Y and chabazite by pentane extraction.

Thermal gravimetric analysis result shows that natural clinoptilolite catalysts crack bitumen into lighter components than thermal cracking or catalytic cracking with other catalysts, including commercial zeolite Y, sodium chabazite and calcium chabazite. This trend is consistent in the liquid hydrocarbon samples extracted using pentane, hexane and toluene. Light hydrocarbons such as pentane or hexane can selectively extract the commercially valuable fractions from the clinptilolite-cracked oilsands samples, leaving the few remaining asphaltenes and other undesirable heavier components in the exhausted sands. This result in the production of lighter and less viscous hydrocarbons and, therefore, more transportable petroleum fractions that contain a higher proportion of fuel-grade hydrocarbons can be produced.

When the vacuum thermal gravimetric results were converted to absolute pressure, it was found that clinoptilolite-catalyzed cracking of oilsands increases the amount of middle distillates while reducing the amount of residual heavy hydrocarbons in bitumen. Thermal and zeolite Y-catalyzed cracking break down the fewest heavier molecules to lighter components, while the cracking performance of chabazite is intermediate.

Natural clinoptilolites cracking also removes a higher portion of contaminants such as nitrogen, sulfur, vanadium and nickel form the raw bitumen. About 24% of total nitrogen, 27% of total sulfur and 59% of vanadium content was removed into gas products or left in exhausted sands. Light hydrocarbons such as pentane or hexane can selectively extract the commercially valuable fractions from the clinoptilolite-cracked samples, leaving the undesirable contaminants in the exhausted sands.

## 4.3 Prospect for future work

This preliminary study investigated natural zeolite-catalyzed cracking assisted light hydrocarbon extraction bitumen from oilsands, which is a step towards in-situ upgrading and waterless bitumen extraction process. Several natural zeolites were tested as cracking agents to crack the oilsands bitumen. Less viscous, lower boiling point liquid hydrocarbon products with fewer contaminants were obtained with high recovery. Since this work is preliminary, some related areas and further accurate quantification is required.

For the catalysis, some natural zeolite properties related to catalytic cracking need further study. For example, the catalysts total number of acid sites, how those sites are

81

distributed on the surface and the acidic strength of catalysts all need to be accurately quantified. The natural zeolite catalytic cracking mechanism and associated chemical reactions need to be investigated.

In relation to the reaction, the process mass and hydrocarbon balance, including accurate quantification of gas products, water, liquid hydrocarbons, asphaltene and coke need to be down. The optimal operation conditions for the catalytic cracking of oilsands need to be determined. The parameters which might affect the cracking efficiency may include: catalysts-to-oilsands ratio, catalyst loading method (stirring or not), the reactor void space, reaction temperature, pressure and reaction time.

In addition, a self-extraction system, which ca generate light hydrocarbon solvents produced in-situ from natural zeolite cracking of oilsands must be developed.